

Synthesis, Spectroscopy, and Reactivity of *meso*-Unsubstituted Azuliporphyrins and Their Heteroanalogues. Oxidative Ring Contractions to Carba-, Oxacarba-, Thiacarba-, and Selenacarba-porphyrins[†]

Timothy D. Lash,* Denise A. Colby, Shelley R. Graham, and Sun T. Chaney

Department of Chemistry, Illinois State University, Normal, Illinois 61790-4160

tdlash@ilstu.edu

Received August 23, 2004

This paper reports the first detailed study on *meso*-unsubstituted azuliporphyrins, an important family of porphyrin-like molecules where one of the usual pyrrole rings has been replaced by an azulene subunit. Although the azulene moiety introduces an element of cross-conjugation, zwitterionic resonance contributors with tropylium and carbaporphyrin substructures give azuliporphyrins diatropic character that falls midway between true carbaporphyrins and nonaromatic benziporphyrins. Protonation affords an aromatic dication where this type of resonance interaction is favored due to the associated charge delocalization. Two different “3 + 1” syntheses of *meso*-unsubstituted azuliporphyrins have been developed. Acid-catalyzed reaction of readily available tripyrrane dicarboxylic acids with 1,3-azulenedicarbaldehyde, followed by oxidation with DDQ or FeCl₃, affords good yields of azuliporphyrins. Alternatively, azulene reacted with acetoxymethylpyrroles (2 equiv) in refluxing acetic acid/2-propanol to give tripyrrane analogues, and following a deprotection step, condensation with a pyrrole dialdehyde in TFA–CH₂Cl₂ gave the azuliporphyrin system. The latter approach was also used to prepare 23-thia- and 23-selenaazuliporphyrins. However, reaction of the azulitripyrrane with 2,5-furandicarbaldehyde produced a mixture of three oxacarba-porphyrins in moderate yield. The free base forms of thia- and selenaazuliporphyrins both showed intermediary aromatic character that was considerably enhanced upon protonation. The UV–vis spectra for azuliporphyrins and their heteroanalogues showed four bands between 350 and 500 nm and broad absorptions at higher wavelengths. Addition of TFA gave dications that showed porphyrin-like spectra with Soret bands between 460 and 500 nm. In the presence of pyrrolidine, azuliporphyrins and their heteroanalogues undergo nucleophilic attack on the seven-membered ring to give carbaporphyrin adducts. These systems also undergo oxidative rearrangements under basic conditions with *t*-BuOOH to give benzocarba-porphyrins. The selenaazuliporphyrin afforded two benzoselenacarba-porphyrins, a previously unknown core-modified carbaporphyrin system. The proton NMR spectra for these compounds showed strong diatropic ring currents with the internal CH resonance upfield above –5 ppm, while the *meso*-protons resonated downfield near 10 ppm. The UV–vis spectra were also porphyrin-like and gave strong Soret bands at ca. 440 nm.

Introduction

The porphyrins have attracted the interest of organic chemists for over 100 years due to their widespread occurrence in nature.¹ These “Pigments of Life” fulfill many roles ranging from oxygen transportation (hemoglobin), electron transfer (cytochromes), and oxidations and reductions (peroxidase, catalase, cytochrome oxidase) to light harvesting and photosynthesis (chlorophylls).¹ Synthetic porphyrins have also been investigated for numerous applications including the production of molecular wires,² oxidation catalysts,³ novel optical materi-

als,⁴ and components of molecular-based information storage systems.⁵ Furthermore, porphyrins and related synthetic pigments have medicinal applications and are being used as photosensitizers in photodynamic therapy.⁶ Analogues of the porphyrins are also being increasingly studied, partially due to the expectation that these systems will also possess useful applications.^{7–12} Core-

* To whom correspondence should be addressed.

[†] Conjugated Macrocycles Related to the Porphyrins. 38. For part 37, see: Richter, D. T.; Lash, T. D. *J. Org. Chem.* **2004**, *69*, in press 8842–8850.

(1) *The Porphyrin Handbook*; Kadish, K. M., Smith, K. M., Guillard, R., Eds.; Academic Press: San Diego, 2000; Vols. 1–10; 2003; Vols. 11–20.

(2) Crossley, M. J.; Burn, P. L. *J. Chem. Soc., Chem. Commun.* **1991**, 1569.

(3) Ostovic, D.; Bruce, T. C. *Acc. Chem. Res.* **1992**, *25*, 314.

(4) Fabian, J.; Nakazumi, H.; Matsuoka, M. *Chem. Rev.* **1992**, *92*, 1197.

(5) Liu, Z.; Yasseri, A. A.; Lindsey, J. S.; Bocian, D. F. *Science* **2003**, *302*, 1543.

(6) (a) Pandey, R. K.; Zheng, G. In *The Porphyrin Handbook*; Kadish, K. M., Smith, K. M., Guillard, R., Eds.; Academic Press: San Diego, 2000; Vol. 6, pp 157–230. (b) Bonnett, R. *Chem. Soc. Rev.* **1995**, *24*, 19.

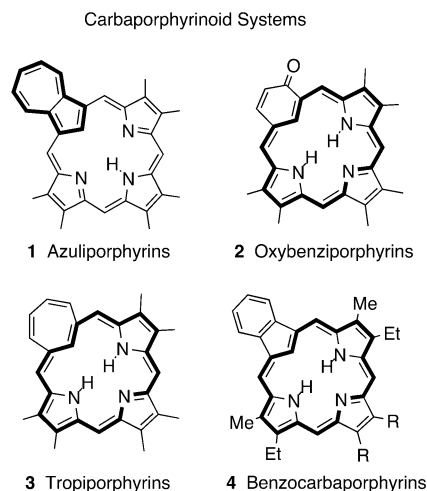
(7) Vogel, E. J. *Heterocycl. Chem.* **1996**, *33*, 1461.

(8) Sessler, J. L. *J. Porphyrins Phthalocyanines* **2000**, *4*, 331.

modified porphyrins where one or more of the nitrogen atoms have been replaced by oxygen, nitrogen, selenium, or tellurium have been known since the late 1960s,¹³ and these systems show unique coordination chemistry¹² as well as some promise as photosensitizers.¹⁴ Carbaporphyrinoid systems, porphyrin analogues where one or more of the pyrrole units have been replaced by carbocyclic rings, were first investigated in the mid-1990s.^{10,11,15–21} These relatively new porphyrin-like macrocycles show somewhat more divergent chemistry, including the formation of stable organometallic derivatives^{21–27} and unprecedented oxidation reactions.^{28,29}

Azuliporphyrins **1** (Chart 1) are a particularly interesting group of carbaporphyrinoids that incorporate an azulene subunit.³⁰ These porphyrin analogues show some overall aromatic character, but this is diminished compared to similar carbaporphyrinoid systems such as oxybenzporphyrins (**2**),¹⁵ tropiporphyrins (**3**),¹⁶ and benzocarbazoporphyrins (**4**)¹⁷ due to cross-conjugation interrupting the 18 π electron delocalization pathway. Azuliporphyrins have been shown to exhibit rich and unusual chemistry^{29,31} and readily form organometallic derivatives with nickel(II), palladium(II), or platinum(II) salts.²⁵

CHART 1



Although the first synthesis of an azuliporphyrin was published in 1997,^{30a} details on the synthesis and spectroscopic properties of these intriguing porphyrinoids and related core-modified systems have not previously been available. In this paper, syntheses of *meso*-unsubstituted azuliporphyrins by two different “3 + 1” methodologies are reported, and this chemistry has also been applied to the preparation of related 23-thia- and 23-selenazuliporphyrins.³⁰ In addition, oxidative ring contractions are shown to give carbaporphyrins, 23-oxacarbaporphyrins, 23-thiacarbaporphyrins, and 23-selenacarbaporphyrins. These studies provide the foundations for future studies in this area of porphyrin analogue chemistry.^{30,32}

Results and Discussion

“3 + 1” Syntheses of Azuliporphyrins. The full potential of the “3 + 1” variant of the MacDonald condensation for porphyrin synthesis had not been appreciated until the mid-1990s.^{33–37} This route involves the condensation of a tripyrrane (e.g., **5**, Scheme 1) with pyrrole dialdehydes to afford, following an oxidation step, the corresponding porphyrin products.³³ This approach is ideally suited for the synthesis of porphyrin analogues with one exotic subunit replacing a pyrrole ring because simple aromatic dialdehydes can be reacted with readily available tripyrranes to give macrocyclic products.^{10,11} Hence, reaction of tripyrranes with 4-hydroxybenzene-1,3-dicarbaldehyde affords oxybenzporphyrins **2**,¹⁵ 1,3,5-cycloheptatriene-1,6-dicarbaldehyde gives tropiporphy-

(9) (a) Sessler, J. L.; Gebauer, A.; Vogel, E. In *The Porphyrin Handbook*; Kadish, K. M., Smith, K. M., Guillard, R., Eds.; Academic Press: San Diego, 2000; Vol. 2, pp 1–54. (b) Sessler, J. L.; Seidel, D. *Angew. Chem., Int. Ed.* **2003**, *42*, 5134.

(10) Lash, T. D. *Synlett* **2000**, 279.

(11) Lash, T. D. In *The Porphyrin Handbook*; Kadish, K. M., Smith, K. M., Guillard, R., Eds.; Academic Press: San Diego, 2000; Vol. 2, pp 125–199.

(12) Latos-Grazynski, L. In *The Porphyrin Handbook*; Kadish, K. M., Smith, K. M., Guillard, R., Eds.; Academic Press: San Diego, 2000; Vol. 2, pp 361–416.

(13) Johnson, A. W. In *Porphyrins and Metalloporphyrins*; Smith, K. M., Ed.; Elsevier: Amsterdam, 1975; pp 729–754.

(14) Hilmey, D. G.; Abe, M.; Nelen, M. I.; Stilts, C. E.; Baker, G. A.; Baker, S. N.; Bright, F. V.; Davies, S. R.; Gollnick, S. O.; Oseroff, A. R.; Gibson, S. L.; Hilf, R.; Detty, M. R. *J. Med. Chem.* **2002**, *45*, 449.

(15) (a) Lash, T. D. *Angew. Chem., Int. Ed. Engl.* **1995**, *34*, 2533. (b) Lash, T. D.; Chaney, S. T.; Richter, D. T. *J. Org. Chem.* **1998**, *63*, 9076. (c) Richter, D. T.; Lash, T. D. *Tetrahedron* **2001**, *57*, 3659.

(16) Lash, T. D.; Chaney, S. T. *Tetrahedron Lett.* **1996**, *37*, 8825.

(17) (a) Lash, T. D.; Hayes, M. J. *Angew. Chem., Int. Ed. Engl.* **1997**, *36*, 840. (b) Lash, T. D.; Hayes, M. J.; Spence, J. D.; Muckey, M. A.; Ferrence, G. M.; Szczepura, L. F. *J. Org. Chem.* **2002**, *67*, 4860. (c) Liu, D.; Lash, T. D. *J. Org. Chem.* **2003**, *68*, 1755.

(18) (a) Berlin, K.; Steinbeck, C.; Breitmaier, E. *Synthesis* **1996**, 336. (b) Berlin, K. *Angew. Chem., Int. Ed. Engl.* **1996**, *35*, 1820.

(19) Hayes, M. J.; Lash, T. D. *Chem. Eur. J.* **1998**, *4*, 508.

(20) Lash, T. D.; Romanic, J. L.; Hayes, M. J.; Spence, J. D. *Chem. Commun.* **1999**, 819.

(21) Miyake, K.; Lash, T. D. *Chem. Commun.* **2004**, 178.

(22) Muckey, M. A.; Szczepura, L. F.; Ferrence, G. M.; Lash, T. D. *Inorg. Chem.* **2002**, *41*, 4840.

(23) Lash, T. D.; Colby, D. A.; Szczepura, L. F. *Inorg. Chem.* **2004**, *43*, 5258.

(24) Lash, T. D.; Rasmussen, J. M.; Bergman, K. M.; Colby, D. A. *Org. Lett.* **2004**, *6*, 549.

(25) (a) Graham, S. R.; Ferrence, G. M.; Lash, T. D. *Chem. Commun.* **2002**, 894. (b) Lash, T. D.; Colby, D. A.; Graham, S. R.; Ferrence, G. M.; Szczepura, L. F. *Inorg. Chem.* **2003**, *42*, 7326.

(26) Stepien, M.; Latos-Grazynski, L.; Lash, T. D.; Sztrenberg, L. *Inorg. Chem.* **2001**, *40*, 6892.

(27) (a) Stepien, M.; Latos-Grazynski, L. *Chem. Eur. J.* **2001**, *7*, 5113. (b) Stepien, M.; Latos-Grazynski, L.; Sztrenberg, L.; Panek, J.; Latajka, Z. *J. Am. Chem. Soc.* **2004**, *126*, 4566. (c) Szymanski, J. T.; Lash, T. D. *Tetrahedron Lett.* **2003**, *44*, 8613.

(28) (a) Hayes, M. J.; Spence, J. D.; Lash, T. D. *Chem. Commun.* **1998**, 2409. (b) Lash, T. D.; Muckey, M. A.; Hayes, M. J.; Liu, D.; Spence, J. D.; Ferrence, G. M. *J. Org. Chem.* **2003**, *68*, 8558.

(29) Colby, D. A.; Ferrence, G. M.; Lash, T. D. *Angew. Chem., Int. Ed.* **2004**, *43*, 1346.

(30) Preliminary communications: (a) Lash, T. D.; Chaney, S. T. *Angew. Chem., Int. Ed.* **1997**, *36*, 839. (b) Graham, S. R.; Colby, D. A.; Lash, T. D. *Angew. Chem., Int. Ed.* **2002**, *41*, 1371.

(31) Lash, T. D. *Chem. Commun.* **1998**, 1683.

(32) These results were presented, in part, at the following meetings: (a) 213th National ACS Meeting, San Francisco, California, April 1997 (Chaney, S. T.; Lash, T. D. *Book of Abstracts*, ORGN 15). (b) 30th Great Lakes Regional American Chemical Society Meeting, Loyola University, Chicago IL, May 1997 (Chaney, S. T.; Lash, T. D. *Program and Abstracts*, Abstract No. 127). (c) 5th Chemical Congress of North America, Cancun, Mexico, Nov 1997 (Lash, T. D.; Chaney, S. T.; Hayes, M. J.; Petryka, J. C.; Richter, D. T. *Book of Abstracts*, Abstract No. 1154). (d) 221st National ACS Meeting, San Diego, CA, April 2001 (Graham, S. R.; Lash, T. D. *Book of Abstracts*, ORGN 186).

(33) Lash, T. D. *Chem. Eur. J.* **1996**, *2*, 1197.

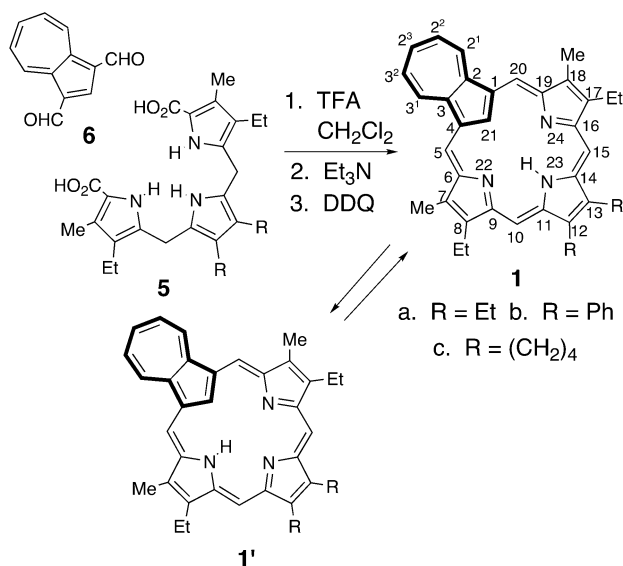
(34) (a) Lin, Y.; Lash, T. D. *Tetrahedron Lett.* **1995**, *36*, 9441. (b) Chandrasekar, P.; Lash, T. D. *Tetrahedron Lett.* **1996**, *37*, 4873.

(35) Lash, T. D. *J. Porphyrins Phthalocyanines* **1997**, *1*, 29.

(36) (a) Boudif, A.; Momenteau, M. *J. Chem. Soc., Chem. Commun.* **1994**, 2069. (b) Boudif, A.; Momenteau, M. *J. Chem. Soc., Perkin Trans. 1* **1996**, 1235.

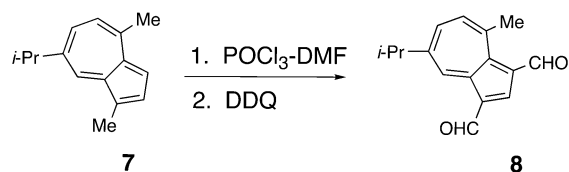
(37) Sessler, J. L.; Genge, J. W.; Urbach, A.; Sanson, P. *Synlett* **1996**, 187.

SCHEME 1

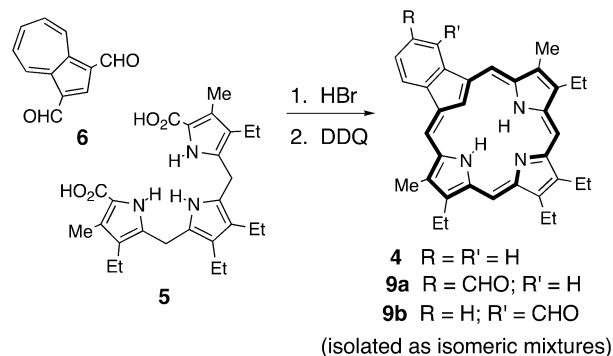


rins **3**,¹⁶ and 1,3-indenedicarbaldehyde yields benzocarbaporphyrins **4** (Chart 1).¹⁷ These aromatic porphyrinoids all show large diatropic ring currents in their proton NMR spectra where the internal CH resonates near -7 ppm. They can also act as trianionic ligands and afford stable silver(III) derivatives.^{22–24} Azulene readily undergoes electrophilic substitution at the 1 and 3 positions and reacts with POCl₃–DMF under Vilsmeier–Haack conditions at 85 °C to give the diformylazulene **6**.³⁸ The 1,3-orientation of the two aldehyde groups provides the correct geometry to generate a carbaporphyrinoid macrocycle. Reaction of **6** with tripyrranes **5** was accomplished with TFA in dichloromethane, and subsequent oxidation with DDQ or aqueous ferric chloride solutions^{39,40} afforded the macrocyclic products **1** (Scheme 1). Column chromatography commonly gave a brown prefraction that appeared to consist of highly impure benzocarbaporphyrin byproducts, and the azuliporphyrins eluted as the solvent polarity was increased as deep green colored bands. Recrystallization was accomplished from chloroform–hexanes and gave the azuliporphyrins as dark green or purple crystals. The azuliporphyrins were only sparingly soluble in organic solvents, and this led to some difficulties in characterizing the free base forms of these porphyrinoids. However, these molecules retained a plane of symmetry by proton NMR spectroscopy, and this indicates that the NH is either favored at position 23 or that the tautomers **1** and **1'** are in rapid equilibrium. The decreased steric interaction between the internal CHs in tautomer **1**, together with the increased potential for hydrogen-bonding interactions, most likely favors this form, and this supposition is supported by DFT studies.⁴¹ We also attempted to synthesize azuliporphyrins from commercially available guaiazulene (**7**). Formylation of **7**, followed by oxidation with DDQ, affords the substituted dialdehyde **8** (Scheme 2).⁴² The presence of two alkyl substituents on the

SCHEME 2



SCHEME 3



azulene ring could potentially increase the solubility of the resulting azuliporphyrins. However, all attempts to react **8** with tripyrrane **5a** failed to give the required porphyrinoid products possibly due to steric interference from the 4-methyl substituent.

During the course of these early investigations, parallel studies were being carried out by Breitmeier and co-workers.^{18a} In this work, dialdehyde **6** was reacted with tripyrrane **5a** in the presence of HBr, and the macrocyclic products were oxidized with DDQ (Scheme 3). These conditions afforded complex mixtures of benzocarbaporphyrins **4** and **9**, and no azuliporphyrin formation was noted in this study.^{18a} Further investigations by our group subsequently showed that this type of rearrangement occurs readily under oxidative conditions (see below).³¹ On the other hand, benzocarbaporphyrins are far more easily synthesized by the reaction of tripyrranes **5** with 1,3-diformylindene, and this direct route also avoids the formation of porphyrinoid mixtures.¹⁷

Although the “3 + 1” approach provides a convenient route to azuliporphyrins, this chemistry is less well suited to the preparation of further modified porphyrinoids with two or more exotic rings. To overcome some of these limitations, the synthesis of a tripyrrane-like system **10** with a central azulene moiety was investigated (Scheme 4).^{30b} Tripyrranes are usually prepared by reacting an α -unsubstituted pyrrole with 2 equiv of an acetoxymethylpyrrole under acidic conditions. This chemistry relies upon the propensity for pyrrole to undergo electrophilic substitution at its α -positions, and indeed, the key carbon–carbon bond-forming steps in most porphyrin syntheses rely upon this property. As azulene favors electrophilic substitution at the equivalent 1,3-positions (Chart 2), we speculated that it might be possible to prepare azulitripyrranes **10** by reacting azulene with acetoxymethylpyrroles **11**. Using mild acidic conditions (refluxing acetic acid/2-propanol), azulene was found to react with 2 equiv of **11a** or **11b** to give good yields of the required tripyrrane analogues. The dibenzyl ester

(38) Hafner, K.; Bernhard, C. *Liebigs Ann. Chem.* **1959**, 625, 108.

(39) Lash, T. D.; Richter, D. T.; Shiner, C. M. *J. Org. Chem.* **1999**, 64, 7973.

(40) Richter, D. T.; Lash, T. D. *Tetrahedron Lett.* **1999**, 40, 6735.

(41) Ghosh, A.; Wondimagegn, T.; Nilsen, H. J. *J. Phys. Chem. B* **1998**, 102, 10459.

(42) Okajima, T.; Kurokawa, S. *Chem. Lett.* **1997**, 69.

SCHEME 4

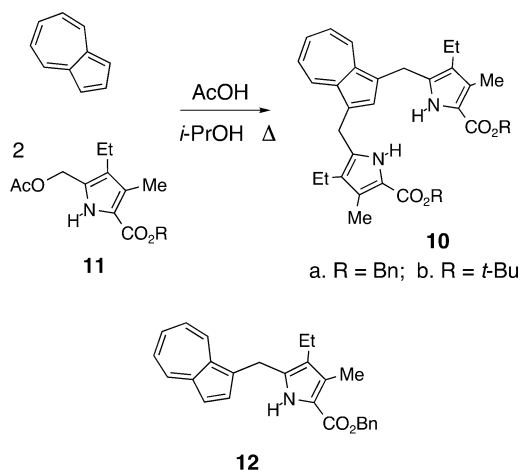
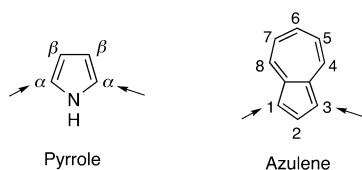


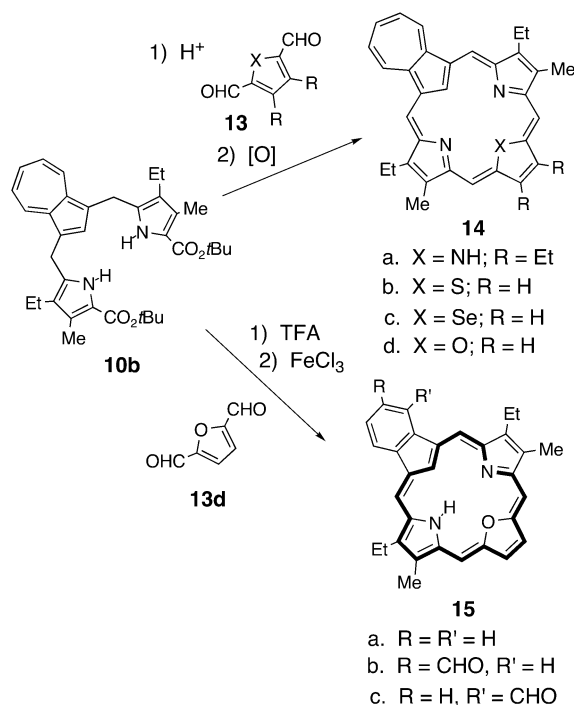
CHART 2



10a precipitates from solution to give a blue powder. The residues were then subjected to column chromatography, and three blue bands were observed corresponding to residual azulene, pyrrolylmethylazulene **12** and azulitripyrrane **10a**. Further recrystallization of the third fraction gave **10a** as blue crystals in a total yield of 73%. When azulene was reacted with 1 equiv of **11a**, the monosubstituted azulene **12** was isolated as the major product. Although the chemistry of **12** is not a topic for this paper, this structure also clearly has potential value in porphyrin analogue synthesis. Reaction of azulene with 2 equiv of *tert*-butyl ester **11b** gave azulitripyrrane **10b** in 59% yield. This product failed to give clear banding on the column, as had been the case for **10a**, but could be isolated reproducibly in pure form. Attempts to cleave the benzyl ester protective groups from **10a** by hydrogenolysis over 10% Pd/C under conventional conditions failed to give the corresponding dicarboxylic acid, and for this reason all of the subsequent studies were performed using the di-*tert*-butyl ester **10b**.

To test the utility of **10b** in macrocycle formation, a “back-to-front” synthesis of the azuliporphyrin system was investigated (Scheme 5). The tripyrrane analogue was initially treated with TFA at room temperature for 10 min to cleave the *tert*-butyl ester protective groups, and then the solution was diluted with dichloromethane and pyrrole dialdehyde **13a** was added. After the mixture was stirred under nitrogen for 2 h, the solution was neutralized with triethylamine and oxidized with DDQ. Following chromatography and recrystallization from chloroform–hexanes, azuliporphyrin **14a** was isolated in 36% yield. This product is an isomer of azuliporphyrin **1a**, and apart from minor differences in the proton NMR spectra, these two compounds are virtually indistinguishable. Reaction of **10b** with 2,5-thiophenedicarbaldehyde (**13b**) similarly afforded the thiaazuliporphyrin **14b**, while diformylselenophene **13c** gave the related selenazuliporphyrin **14c**. For the core-modified azuliporphyrins,

SCHEME 5

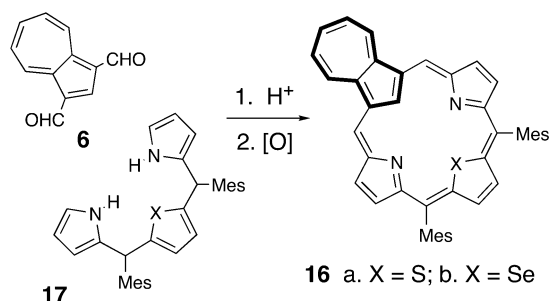


the best results were obtained using 0.1% aqueous ferric chloride solutions as the oxidant, and **14b** and **14c** were isolated in 45% and 27% yields, respectively. Interestingly, 2,5-furandicarbaldehyde (**13d**) failed to give any isolatable oxaazuliporphyrin **14d**, although the oxacarba-porphyrins **15a–c** were isolated in moderate yield instead. Furan-containing porphyrinoids of this type are relatively basic and cannot be isolated as the free base structures.⁴³ Instead, the solutions are washed with dilute hydrochloric acid and the products isolated as the corresponding hydrochloride salts. A related oxacarba-porphyrin has been synthesized from a furan-containing tripyrrane analogue and diformyl indene, and this system has been fully characterized previously.⁴³ For this reason, the properties of **15a–c** will not be discussed in detail. However, it is worth noting that these porphyrinoids show strong diatropic ring currents by proton NMR spectroscopy and the interior CH resonates between -6.4 and -6.8 ppm for solutions in $CDCl_3$. The UV–vis spectra for the free base forms in 5% Et_3N –chloroform closely resembles porphyrin-type chromophores. Oxacarba-porphyrin **15a** shows a Soret band at 430 nm, together with a series of four “Q-bands” at 522, 555, 620, and 681 nm. Oxacarba-porphyrins have been shown to be superior organometallic ligands forming stable nickel(II), palladium(II), and platinum(II) derivatives.⁴³ Azulitripyrrane **10b** has also been used to synthesize a dicarba-porphyrinoid system,^{30b} but full details of this study will be reported elsewhere.

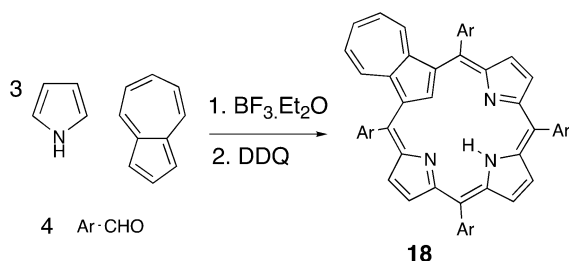
These routes to azuliporphyrins are straightforward and versatile and are starting to see application by other research groups. Recently, Chandrashekar and co-workers have prepared two core-modified azuliporphyrins **16**⁴⁴ by reacting **6** with dimesityltripyrans **17** under the conditions developed by our group for the synthesis of

(43) (a) Liu, D.; Lash, T. D. *Chem. Commun.* **2002**, 2426. (b) Liu, D.; Ferrence, G. M.; Lash, T. D. *J. Org. Chem.* **2004**, 69, 6079.

SCHEME 6



SCHEME 7



Ar = Ph, C₆D₅, *p*-CH₃C₆H₄, *p*-ClC₆H₄,
p-BrC₆H₄, *p*-IC₆H₄, *p*-O₂NC₆H₄, C₆F₅

etioazuliporphyrins **1a–c** (Scheme 6). In addition, the same approach has been applied to the preparation of a tribenzoazuliporphyrin by Okujima et al.⁴⁵ We have also developed a one-pot route to tetraarylazuliporphyrins **18** using Rothemund-type chemistry under Lindsey's boron trifluoride etherate catalyzed conditions (Scheme 7).⁴⁶ This has made it possible to conduct parallel studies on the chemistry of *meso*-unsubstituted and *meso*-tetrasubstituted systems that parallels research into true porphyrins. This approach has been particularly useful for investigations into the metalation of azuliporphyrins²⁵ and related benzocarbaporphyrins.^{22,23}

Aromatic Character, Protonation, and Solvent Effects. The UV–vis spectra of azuliporphyrins **1** show a distinctive set of four bands between 350 and 500 nm followed by a broad band that extends over most of the remaining visible region (Figure 1). These spectra are quite different from the spectra obtained for porphyrins or aromatic carbaporphyrinoids such as oxybenzoporphyrins **2** or benzocarbaporphyrins **4** (Chart 1) which show a strong Soret band near 400 nm and a series of minor Q-bands at longer wavelengths.^{15,17} This suggests that the azuliporphyrin system is electronically quite different from true porphyrins, a property that we attribute to the presence of a cross-conjugated azulene ring. The proton NMR spectra for azuliporphyrins **1a–c** also confirm the reduced aromatic character for this system compared to carbaporphyrinoids **2–4**.^{15–17} For benzocarbaporphyrins **4**, the external *meso*-protons give rise to two 2H singlets near 10 ppm,¹⁷ but the equivalent resonances for **1c** show

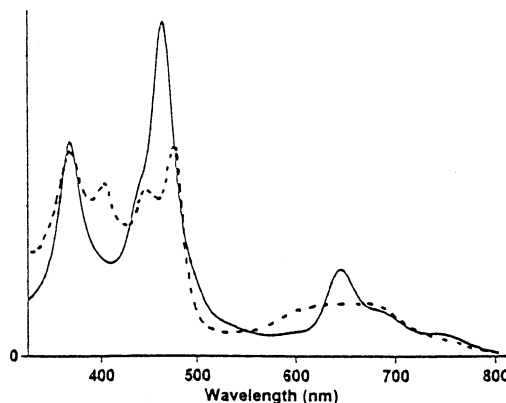
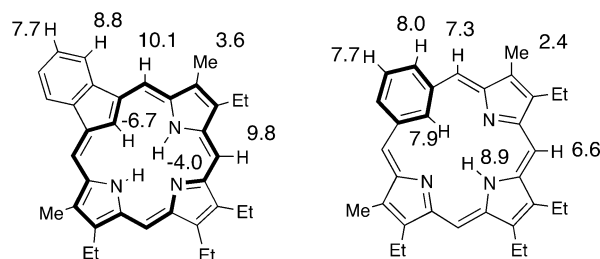


FIGURE 1. UV–vis spectra of diphenylazuliporphyrin **1b**. Dotted line: free base in 5% Et₃N–chloroform. Bold line: dication in 5% TFA–chloroform.

CHART 3^a

4 Benzocarbaporphyrins

19 Benziporphyrin

^a Selected chemical shift values from the proton NMR spectra of benzocarbaporphyrin **4** and benziporphyrin **19**. The aromatic porphyrinoid shows a $\Delta\delta$ between the internal and external protons of nearly 17 ppm, but the overall nonaromatic benziporphyrin shows no significant difference between the chemical shifts for the internal and external benzene protons.

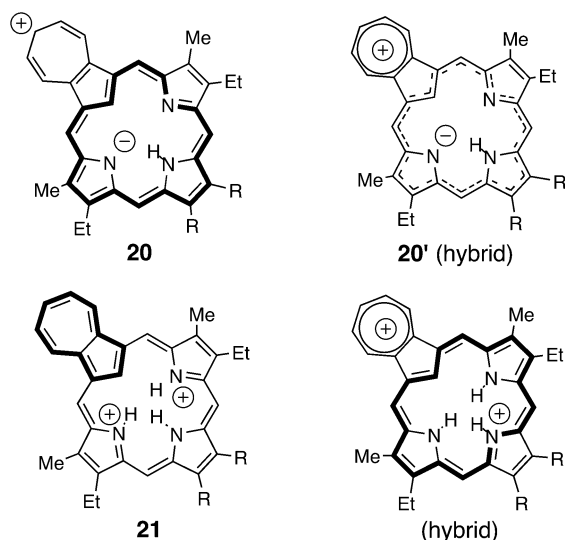
up at 8.9 and 9.2 ppm. Significant problems arise in analyzing the spectra for the free base azuliporphyrins as they have poor solubility characteristics and aggregate in solution. Traces of water seem to decrease the aggregation and improve the quality of the spectra in some cases. The internal CH is difficult to assign because this resonance falls into a region obscured by solvent impurities, and this is particularly problematic for poorly soluble samples of this type. However, azuliporphyrin **1c** gives the best solubility characteristics and produces a broad ¹H resonance at 1.8 ppm in anhydrous CDCl₃ that was distilled from calcium hydride. These results indicate that azuliporphyrins have some aromatic character. While benzocarbaporphyrin shows the internal CH at ca. –7 ppm, the overall nonaromatic benziporphyrin system **19** shows the equivalent resonance at +7.9 ppm (Chart 3).^{15b} The *meso*-protons for **19** are also present at 6.6 and 7.3 ppm.^{15b} Therefore, azuliporphyrins seem to fall into an intermediary region that falls far short of the strongly aromatic character demonstrated by **2** and **4**. These properties are attributed to dipolar resonance contributors such as **20** that can be generalized with the hybrid structure **20'** (Chart 4). The seven-membered ring can donate electron density, thereby taking on tropylium-type character while producing an 18 π electron delocalization pathway within the macrocycle. This produces two aromatic subunits, which is clearly beneficial, but these

(44) Venkatraman, S.; Anand, V. G.; PrabhuRaja, V.; Rath, H.; Sankar, J.; Chandrashekar, T. K.; Teng, W.; Senge, K. R. *Chem. Commun.* **2002**, 1662.

(45) Okujima, T.; Komobuchi, N.; Shimizu, Y.; Uno, H.; Ono, N. *Tetrahedron Lett.* **2004**, 45, 5461.

(46) (a) Colby, D. A.; Lash, T. D. *Chem. Eur. J.* **2002**, 8, 5397. (b) Lash, T. D.; Colby, D. A.; Ferrence, G. M. *Eur. J. Org. Chem.* **2003**, 4533.

CHART 4



dipolar canonical forms are limited due to the requirement for charge separation. Some interesting differences in the chemical shifts can be seen due to solvent, although low solubility restricts this type of investigation. In C_6D_6 , azuliporphyrin **1c** was sufficiently soluble to give a proton NMR spectrum. The *meso*-protons were observed at 7.9 and 8.8 ppm, compared to 7.9 and 8.9 ppm in $CDCl_3$, while the doublet for the azulene protons nearest to the macrocycle shifted upfield from 9.2 ppm in $CDCl_3$ to 8.8 ppm in C_6D_6 . These results suggest that the azuliporphyrin system has a slightly decreased macrocyclic ring current in C_6D_6 compared to $CDCl_3$, possibly due to a lesser degree of stabilization to the dipolar contributors in the less polar hydrocarbon solvent. Pyridine would be expected to stabilize the dipolar resonance contributors and lead to enhanced diatropic character. This appears to be the case, as the *meso*-protons for **1c** in C_5D_5N resonate at 8.3 and 9.4 ppm, while the 2H azulene doublet appears at 9.6 ppm. Unfortunately, the internal CH could not be observed in these studies, although similar trends were obtained for thia- and selenazuliporphyrins **14b** and **14c**. It is worth noting that *meso*-tetraphenylazuliporphyrin **18** gives the internal CH resonance at +3.2 ppm, but in this case the phenyl groups are likely to decrease the planarity of the macrocycle due to steric interactions and this provides an explanation for the observed downfield shift of this resonance compared to **1c**.

Azuliporphyrins readily protonate to give the corresponding dications **21** (Chart 4). The UV-vis spectrum of **1b** in TFA-chloroform is far more porphyrin-like showing two strong Soret-like bands at 368 and 466 nm and more defined Q-type bands at higher wavelengths (Figure 1). Electron-donation from the cycloheptatriene ring can now aid in charge delocalization, and this more strongly favors a combination of tropylium and carba-porphyrin character in the dications. This leads to a pronounced increase in the diatropic ring current for the diprotonated species. For instance, the 400 MHz proton NMR spectrum of diphenylazuliporphyrin **1b** in TFA- $CDCl_3$ shows the internal CH at -3 ppm, while the NHs resonate between 0 and -2 ppm (Figure 2). The *meso*-protons are shifted downfield giving two 2H singlets at

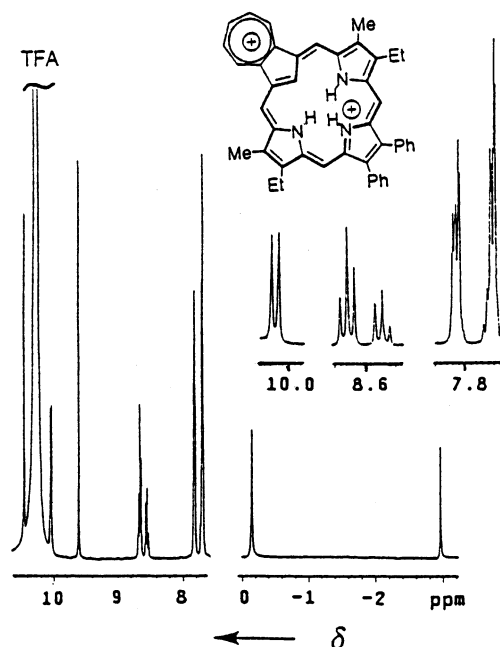


FIGURE 2. Partial 400 MHz proton NMR spectrum of diphenylazuliporphyrin **1b** in TFA- $CDCl_3$. This spectrum corresponds to the aromatic dication.

9.6 and 10.5 ppm, while the 2H azulene doublet is also downfield at 10.0 ppm.

Core-modified azuliporphyrins **14b** and **14c** show many of the same characteristics exhibited by **1a-c**. The UV-vis spectrum for thiaazuliporphyrin **14b** in 5% Et_3N -chloroform also shows four bands in the near-UV and blue regions at λ_{max} values of 372, 384, 448, and 477 nm, followed by broad absorptions between 500 and 800 nm. Selenazuliporphyrin **14c** gave four defined bands at 363, 399, 449, and 476 nm, again followed by broad ill-defined absorptions at longer wavelengths. The spectra are all superficially similar, although the first two bands in the UV-vis spectrum for **14b** are starting to merge together. The proton NMR spectrum for **14b** in $CDCl_3$ showed the *meso*-protons downfield at 9.0 and 9.2 ppm, suggesting a slightly increased diatropic character, while the thiophene protons gave a singlet at 8.8 ppm and the azulene doublet was present at 9.5 ppm. However, the internal CH could be identified at 2.8 ppm, a value that is significantly downfield from the broad resonance observed for **1c**. In C_6D_6 , the *meso*-protons resonated at 8.8 and 9.1 ppm, while the thiophene ring gave a 2H singlet at 8.5 ppm and the azulene doublet appeared at 8.9 ppm. In pyridine- d_5 , the equivalent resonances were observed at 9.4, 9.8, 9.1, and 10.0 ppm, respectively. These values suggest that the diatropic character arising from dipolar resonance contributors is slightly enhanced in pyridine and slightly diminished in benzene. Unfortunately, the low solubility of **14b** in C_6D_6 prevented us from identifying the internal CH resonance. In C_5D_5N , the internal CH gave a 1H singlet at 3.2 ppm which seemingly contradicts the trends observed for the external protons. In the proton NMR spectrum for selenazuliporphyrin **14c** in $CDCl_3$ (Figure 3), the two 2H *meso*-resonances were observed near 9.2 ppm, while the selenophene unit gave a 2H singlet at 8.9 and the azulene $2^1,3^1$ -protons produced a 2H doublet at 9.5 ppm. In

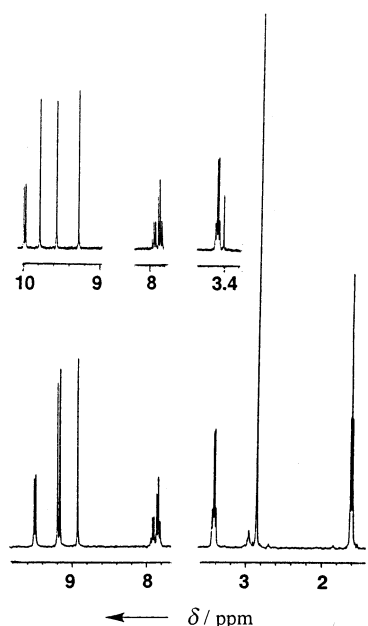
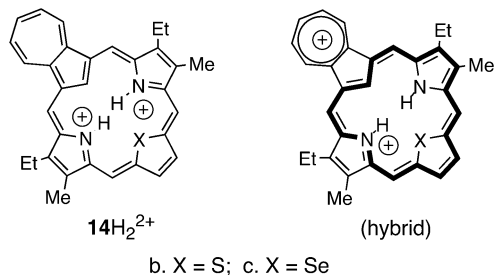


FIGURE 3. 400 MHz proton NMR spectra of selenazuliporphyrin **14c**. The lower spectrum was run in CDCl_3 . The small broad peak near 3 ppm corresponds to the internal CH, while the three singlets around 9 ppm represent the selenophene and *meso*-protons. The upper spectrum corresponds to **14c** in pyridine- d_5 . The external protons are significantly shifted downfield, suggesting an increased macrocyclic ring current, but the internal CH is also shifted downfield and gives a sharp singlet at 3.4 ppm.

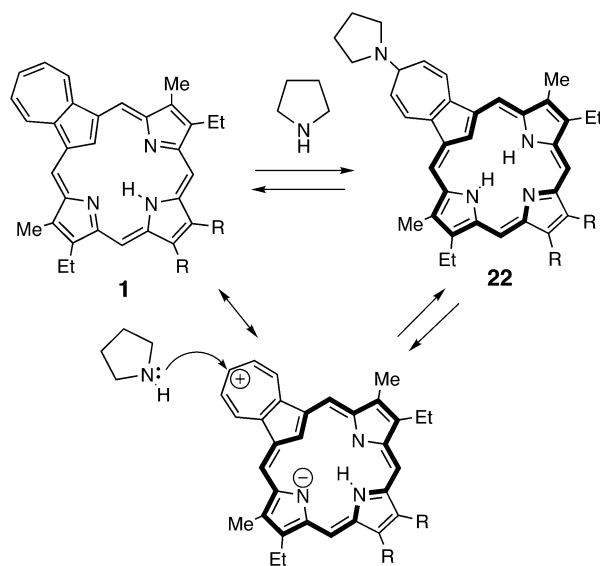
CHART 5



benzene- d_6 , these resonances were present at 8.9, 9.0, 8.7, and 9.1 ppm, showing a decreased ring current, while pyridine- d_5 showed increased diatropicity with equivalent resonances at 9.6, 9.8, 9.3, and 10.0 ppm, respectively. Again, the internal CH resonance did not agree with this trend and gave 1H resonances at 3.0, 3.5, and 3.4 ppm in CDCl_3 , C_6D_6 , and $\text{C}_5\text{D}_5\text{N}$, respectively. The results for the external protons are consistent and suggest that the thia- and selenazuliporphyrins have comparable diatropic character that is enhanced in pyridine but slightly diminished in benzene. The chemical shift values for the internal CH is most likely effected by subtle steric and conformational factors, and these values provide a poorer guide to the overall diatropicity of these systems.

Addition of TFA to solutions of **14b** or **14c** in chloroform affords the corresponding dications 14H_2^{2+} (Chart 5). These dications would be expected to take on greater overall aromatic character due to favorable charge delocalization as was the case for **1a–c**. The UV–vis spectrum of **14b** in TFA–chloroform is more porphyrin-like, showing a Soret band at 468 nm and a weaker absorption

SCHEME 8



at 385 nm. The selenophene analogue **14c** shows a strong band at 494 nm and two weak bands near 380 nm. The UV–vis spectra for the dications derived from **1**, **14b**, and **14c** show an increasing dominance for the stronger Soret-like band compared to the other absorptions going from NH to S to Se. The proton NMR spectra for **14b** and **14c** in TFA– CDCl_3 show strong ring currents with the internal CH at -3.4 ppm for **14b** and -2.6 ppm for **14c**. The small difference between these values does not seem to be significant as the chemical shift values for the external protons are comparable. Carbon-13 NMR spectra for **13b** and **13c** confirm the presence of a plane of symmetry in these macrocycles.

Nucleophilic Additions and Oxidative Ring Contractions. Azuliporphyrins are susceptible to nucleophilic attack onto the electron-deficient cycloheptatriene ring, and this reactivity may play a role in the oxidative ring contraction of azuliporphyrins to afford benzocarpophyrins. Addition of excess pyrrolidine to solutions of **1a** in chloroform leads to the reversible formation of the pyrrolidine adduct **22a** (Scheme 8).³¹ This process is an equilibrium and removal of the excess pyrrolidine leads to the reformation of azuliporphyrin **1a**. On addition of pyrrolidine, the solutions turn from a deep green to a dark brown color that is typical of carboxyporphyrin systems. In the presence of increasing amounts of pyrrolidine, a Soret-like band emerges near 400 nm, and Q type bands appear between 500 and 700 nm.³¹ The pyrrolidine adduct has a true carboxyporphyrin delocalization pathway and this leads to a strong diatropic ring current in the proton NMR spectra. In pyrrolidine- d_8 – CDCl_3 , **22a** gives a 1H singlet for the internal CH at -6.9 ppm, while the external *meso*-protons resonate downfield at 9.7 and 9.9 ppm (Figure 4). The symmetry of the system is evident from the simplicity of the spectrum, confirming that the pyrrolidine attacks the carbon atom furthest removed from the porphyrinoid macrocycle. It should be noted that the observed adduct is the thermodynamic product resulting from the equilibrium, and nucleophilic attack may well also occur at other positions on the cycloheptatriene ring. The alkene units of the seven-membered ring give rise to a two 2H doublet of doublets at 6.0 and 7.8 ppm. The latter resonance is

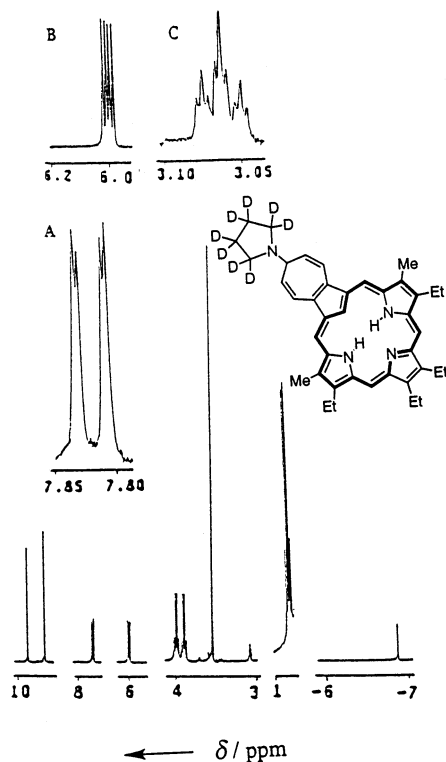
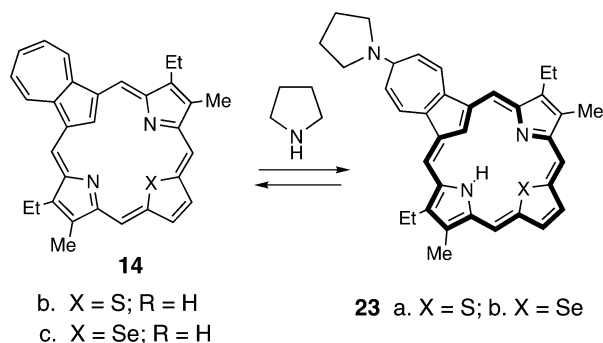


FIGURE 4. 400 MHz proton NMR spectrum of **1a** in CDCl_3 with one drop of pyrrolidine- d_8 . The resulting adduct shows strongly diatropic character with the internal CH near -7 ppm. Insets A–C show details for the protons on the seven-membered ring.

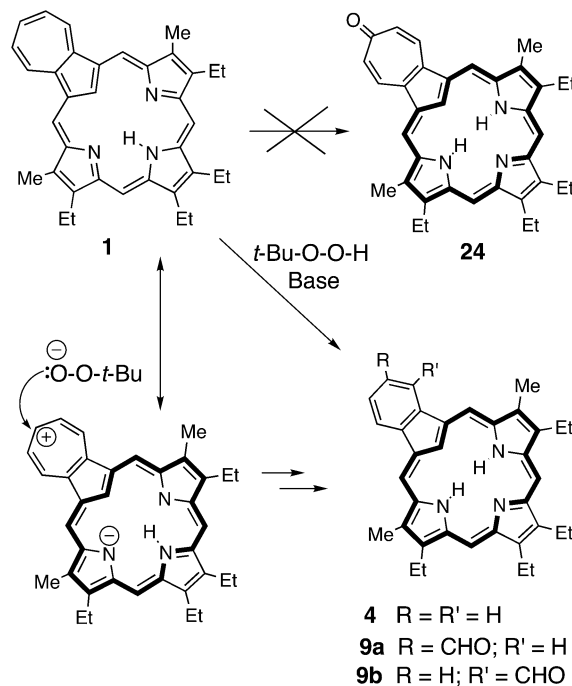
shifted downfield due to the proximity of the 2^1 and 3^1 protons to the 18π electron delocalization pathway. The CH connected to the pyrrolidine nitrogen gave a 1H triplet of triplets at 3.1 ppm. The porphyrin methyl substituents resonated at 3.5 ppm as would be expected for a species of this type with a fully aromatic porphyrinoid ring current.

Tetraarylazuliporphyrins **18** (Scheme 7) also form adducts of this type with pyrrolidine, although trace amounts of the 2° amine are sufficient to form this type of species for this series. The formation of these adducts may be more favored in the *meso*-tetrasubstituted porphyrinoids due to relief of steric congestion between the seven-membered ring and the adjacent aryl substituents. Thiaazuliporphyrin **14b** also affords a pyrrolidine adduct **23a**, but this requires a much larger excess of pyrrolidine to drive the equilibrium (Scheme 9). Although the addition of one drop of pyrrolidine to 1 mg of **1a** in CDCl_3 was sufficient to completely form the adduct **22**, 10 drops were required to fully generate the corresponding core-modified adduct **23a**. The proton NMR spectrum was similar to the one obtained from **1a**, and the internal CH was noted at -5.4 ppm for the thiaazuliporphyrin. Selenazuliporphyrin **14c** also gave the corresponding adduct **23b**, but even larger proportions of pyrrolidine were required in this case. Addition of 20 drops of pyrrolidine- d_8 to the NMR tube gave a spectrum where the adduct predominated, and in this case the internal CH resonated at -4.7 ppm. The larger sulfur and selenium atoms may reduce the favorability of the carbaporphyrinoid adduct by decreasing the planarity of the macrocyclic core. However, the same type of chem-

SCHEME 9



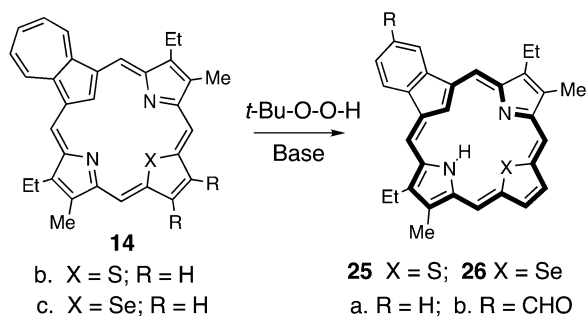
SCHEME 10



istry can occur to a greater or lesser extent for all of the azuliporphyrin systems.

The ability for azuliporphyrins to undergo nucleophilic attack suggested that further chemistry may be possible to form modified porphyrinoid structures. Under alkaline conditions, azuliporphyrin **1a** was reacted with *tert*-butyl hydroperoxide in an attempt to generate the tropone derivative **24** (Scheme 10).³¹ We had speculated that nucleophilic attack by the *tert*-butyl hydroperoxide anion, followed by elimination of *tert*-butyl alcohol, would afford **24**.³¹ However, these reaction conditions gave benzocarbazoporphyrin products **4** and **9** instead. Using KOH as the base in methanol–dichloromethane, **1a** reacted with *t*-BuOOH to give benzocarbazoporphyrin **4** as the major product in 31% yield. However, when the reaction was performed using potassium *tert*-butoxide as the base, two major carbaporphyrin products were isolated. Following chromatography and recrystallization, **4** was isolated in 19% yield together with a 35% yield of the formyl derivative **9a**. A third minor fraction was noted that was tentatively assigned as the isomeric aldehyde **9b**. The chemistry provides an alternative entry into benzocarbazoporphyrin systems, and this approach has been applied to the synthesis of *meso*-tetraarylbenzocarbazoporphyrins.⁴⁶

SCHEME 11



Detailed mechanisms to explain this chemistry involving a nucleophilic addition, Cope rearrangement, elimination process has been proposed elsewhere.^{31,46b} A similar process was presumably responsible for Breitmeier's results,^{18a} as well as the formation of oxacarba-porphyrins in the "3 + 1" chemistry using 2,5-furandicarbaldehyde (Scheme 5). It was of additional interest to see whether this chemistry also occurred for the core-modified azuliporphyrins **14b** and **14c**. Treatment of **14b** with $t\text{-BuOOH}$ in the presence of KOH gave thiacarba-porphyrin **25a** in 9.5% yield (Scheme 11). The carba-porphyrinoid gave a porphyrin-like UV-vis spectrum in 1% $\text{Et}_3\text{N-CHCl}_3$ with a Soret band at 434 nm. The proton NMR spectrum for **21a** in CDCl_3 showed the inner CH as a singlet at -5.90 , the NH resonance as a broad peak at -5.08 and the *meso*-protons as two 2H singlets near 10.1 ppm, values that confirm the presence of a powerful diatropic ring current. When the reaction of **14b** with $t\text{-BuOOH}$ was performed in the presence of $t\text{-BuOK}$, a mixture of **25a** and aldehyde **25b** were isolated in approximately 50% yield. These were generated in a 2:1 ratio, where the aldehyde predominated, but the two products proved to be virtually impossible to separate. The same differences in reaction selectivity clearly applies to the thiaazuliporphyrin system, again emphasizing the similarities between **1a** and **14b**. However, a similar thiacarba-porphyrin has been synthesized by a rational "3 + 1" route and the properties of this system investigated in detail.⁴³ For this reason, the chemistry was not further pursued for thiaazuliporphyrin **14b**. Reactions of $t\text{-BuOOH}$ with selenazuliporphyrin **14c** gave similar results (Scheme 11). Using $t\text{-BuOK}$, **14c** gave selenacarba-porphyrin **26a** in 10% yield. However, using KOH as the base, **14c** afforded two major products: **26a** (16%) and the related aldehyde **26b** (22%). In this case the two major products could be separated by flash chromatography and fully characterized.

Selenacarba-porphyrins have not previously been synthesized and this new porphyrin analogue system was further investigated. Due to the relative simplicity of the spectra for **26a**, the discussion will emphasize this compound over the related asymmetrical aldehyde. However, apart from the obvious structural differences, the two selenacarba-porphyrins gave similar spectroscopic data. In 1% $\text{Et}_3\text{N-CHCl}_3$, **26a** gave a porphyrin-like spectrum with a relatively broad Soret band at λ_{max} 436 nm and three weaker absorptions between 500 and 650 nm (Figure 5A). The proton NMR spectrum for **26a** in CDCl_3 showed a singlet for the internal CH at -5.4 ppm and a broad resonance for the NH at -4.9 ppm (Figure 5B). The strong diatropic ring current is confirmed by

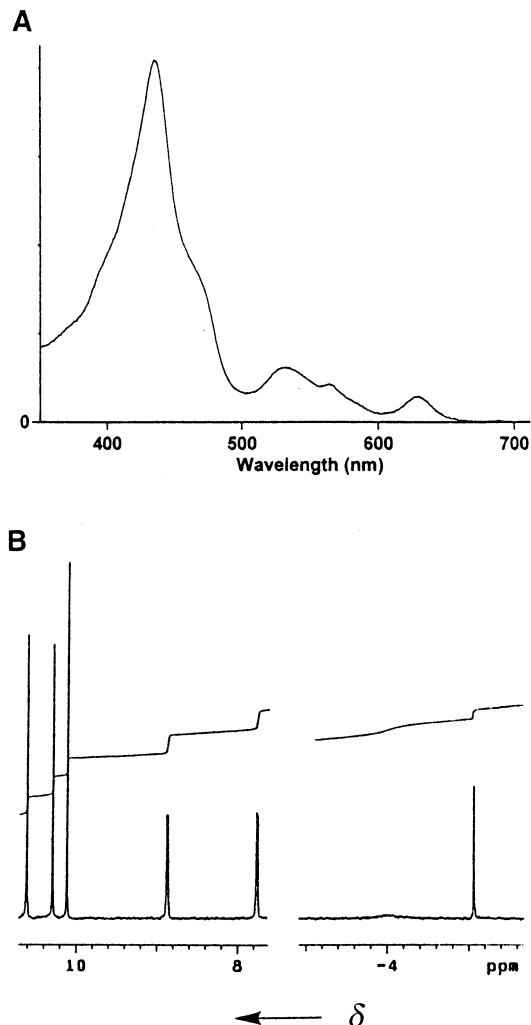
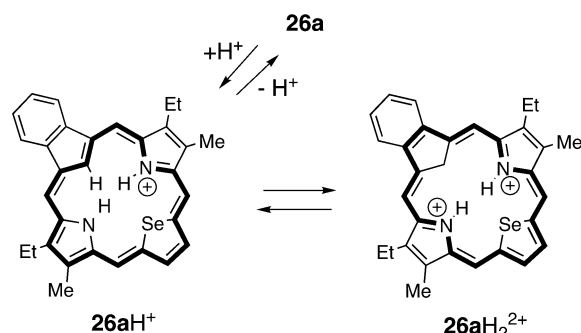


FIGURE 5. (A) UV-vis spectrum of 23-selena-21-carba-porphyrin **26** in 1% $\text{Et}_3\text{N-CHCl}_3$ showing porphyrin-like characteristics with a broadened Soret band at 436 nm. (B) Partial 400 MHz proton NMR spectrum of **26** in CDCl_3 showing the upfield and downfield regions. The internal CH is present as a sharp singlet at -5 ppm, while the NH gives a broad resonance near -4 ppm. The *meso*- and selenophene protons give rise to three 2H singlets downfield below 10 ppm.

the presence of two downfield 2H singlets for the *meso*-protons at 10.2 and 10.4 ppm. The selenophene protons also gave a downfield 2H singlet at 10 ppm, while the methyl substituents showed the indirect effect of the diatropic ring current giving rise to a 6H singlet at 3.4 ppm. These results show that the diatropicity of thia- and selenacarba-porphyrins is not significantly different from benzocarba-porphyrins **4**. Both **25** and **26** give NMR spectra that show an apparent plane of symmetry, although the presence of a single NH proton means that this must be due the averaging of two equivalent tautomeric forms due to rapid NH exchange. Addition of trace TFA gave the related monocation **26H⁺** (Scheme 12), and the UV-vis spectrum for this species in 0.1% TFA- CHCl_3 gave a Soret band at 469 nm. At higher acid concentrations, minor shifts were observed but these spectra all appeared to correspond to **26H⁺**. The proton NMR spectrum of **26H⁺** in TFA- CDCl_3 gave a 1H singlet for the interior CH at -5.6 ppm and a 2H broad peak at -4.3 ppm for the NH's. The *meso*-protons shifted down-

SCHEME 12



field to give two 2H resonances at 10.4 and 11.0 ppm, while the selenophene protons gave a 2H singlet at 10.1 ppm and the methyl groups afforded a 6H resonance at 3.6 ppm. Taken together, these data indicate that the ring current is slightly larger for the protonated structure. Addition of TFA-*d* to a solution of **26a** in CDCl₃ showed the immediate disappearance of the internal CH and NH resonances. This indicates that a C-protonated dication **26aH₂²⁺** is present in equilibrium with the monocation **26aH⁺** (Scheme 12). Similar C-protonated cations have been observed for carbaporphyrins¹⁷ and related systems.^{20,47} Over a period of 1 week at room temperature, some loss of signal intensity for the peaks at 10.4 and 11.0 ppm was noted indicating that slow exchange was also occurring at the *meso*-positions. This may be due to low concentrations of *meso*-C-protonated species similar to those previously proposed for carbaporphyrins **4**.¹⁷

Conclusions

Azuliporphyrins are easily synthesized by reacting 1,3-azulenedicarbaldehyde with tripyrranes under conventional “3 + 1” conditions. Alternatively, azulene analogues of the tripyrranes can be constructed by reacting acetoxymethylpyrroles with azulene under mildly acidic conditions, and following deprotection of the terminal ester groups, reaction with a pyrrole dialdehyde gives the azuliporphyrin system. This alternative “3 + 1” approach has the advantage of making related core-modified azuliporphyrins easily accessible. Hence, reaction of the azulitripyrrane with thiophene and selenophene dialdehydes affords the related thia- and selenazuliporphyrins in good yields. Although 2,5-furandicarbaldehyde failed to give an oxazuliporphyrin, a series of oxacarbaporphyrins were generated instead. Azuliporphyrins and their core-modified analogues show intermediary diatropic character falling midway between the nonaromatic benziporphyrin system and the highly diatropic carbaporphyrins. The intermediary porphyrinoid aromaticity derives from dipolar resonance contributors that have a carbaporphyrinoid core and a peripheral fused tropylium cation. Protonation greatly enhances the diatropicity because this type of canonical form now aids in charge delocalization. Azuliporphyrins, thiaazuliporphyrins, and selenazuliporphyrins all form carbaporphyrin adducts in the presence of excess pyrrolidine due to reversible nucleophilic attack onto the cycloheptatriene ring. This

reactivity is also believed to be responsible for the oxidative ring contraction of azuliporphyrins and heteroazuliporphyrins to give carbaporphyrins in the presence of alkaline solutions of *tert*-butyl hydroperoxide. This study provides efficient routes to the *meso*-unsubstituted azuliporphyrins and makes available details of their spectroscopic and chemical properties that will facilitate future investigations in this area.

Experimental Section

1,3-Azulenedicarbaldehyde (6). Prepared by the Vilsmeier formylation of azulene (500 mg) using the procedure of Hafner and Bernhard³⁸ as burgundy needles (376 mg, 52%): mp 190–191 °C (lit.³³ mp 190 °C); ¹H NMR (CDCl₃) δ 7.96 (2H, t, *J* = 10 Hz), 8.15 (1H, t, *J* = 9.8 Hz), 8.64 (1H, s), 9.89 (2H, d, *J* = 9.6 Hz), 10.35 (2H, s); ¹³C NMR (CDCl₃) δ 126.1, 134.2, 140.9, 142.8, 144.5, 148.7, 187.3.

2,5-Selenophenedicarbaldehyde (13c). A mixture of selenophene (2.50 g), TMEDA (2.712 g) and hexanes (6 mL) was placed in a three neck round-bottom flask equipped with a thermometer, a condenser, and a rubber septum. The vessel was flushed with nitrogen for ca. 7 min, and the mixture cooled to –5 °C with the aid of a salt–ice bath. A solution of *tert*-butyllithium in pentane (1.5 M, 26 mL) was slowly added via a syringe to the stirred mixture while maintaining the temperature <5 °C. After the addition had been completed, the solution was allowed to warm to room temperature and then refluxed for 30 min. Freshly distilled THF (23 mL) was added, and the solution cooled to –40 °C. DMF (5.60 g) was added over a period of 10 min. After the addition had been completed, the solution was allowed to warm to room temperature and was stirred for a further 30 min. The solution was poured into a mixture of concentrated hydrochloric acid (31 mL) in water (325 mL) at –5 °C, and the pH was adjusted to a value of 6 with saturated sodium bicarbonate solution. The solution was extracted with ether (4 × 250 mL), and the combined ether extracts were dried over sodium sulfate. The solvent was evaporated and the residue recrystallized from ethanol. The crystals were dried in vacuo overnight to give the dialdehyde (2.18 g, 61%) as pale brown crystals: mp 85 °C (lit.⁴⁸ mp 83 °C); ¹H NMR (CDCl₃) δ 8.11 (2H, s), 9.89 (2H, s); ¹³C NMR (CDCl₃) δ 138.4, 156.3, 185.0.

Benzyl 5-(1-Azulenylmethyl)-4-ethyl-3-methylpyrrole-2-carboxylate (10a) and 1,3-Bis(5-benzoyloxycarbonyl-3-ethyl-4-methyl-2-pyrrolylmethyl)azulene (12). Azulene (85 mg) and benzyl 5-acetoxymethyl-4-ethyl-3-methylpyrrole-2-carboxylate⁴⁹ (427 mg) were dissolved in 2-propanol (10 mL) and acetic acid (1 mL). The mixture was flushed with nitrogen and stirred under reflux overnight. The solution was allowed to cool to room temperature and cooled in the freezer for 1 h. The precipitate was filtered and washed with ethanol to give the tripyrrane analogue (195 mg, 46%) as a blue powder. The filtrate was evaporated to dryness on a rotary evaporator and the residue chromatographed on silica eluting initially with 50% hexanes–dichloromethane and then gradually increasing the proportion of dichloromethane to 100%. Initially a small blue fraction containing azulene was collected, followed by a blue band corresponding to the monopyrrolic product **12**, and finally the tripyrrane analogue **10a** eluted as a deep blue fraction. Compound **12** was recrystallized from ethanol to give dark blue crystals (9 mg, 3.5%), while **10a** recrystallized from ethanol to afford blue crystals (115 mg, overall yield 73%). In some experiments where the reaction temperature was barely sufficient to achieve reflux, a higher proportion of byproduct **12** was observed. When azulene (85 mg) was reacted with 1 equiv of acetoxymethylpyrrole **11a** (210 mg) under the same

(48) Paulmier, C.; Pastour, P. *Bull. Soc. Chim. Fr.* **1966**, 4021.

(49) Johnson, A. W.; Kay, I. T.; Markham, E.; Price, R.; Shaw, K. *B. J. Chem. Soc.* **1959**, 3416.

(47) Lash, T. D.; Richter, D. T. *J. Am. Chem. Soc.* **1998**, *120*, 9965.

conditions, **12** was isolated as the major reaction product and afforded dark blue crystals (125 mg, 49%) after recrystallization from ethanol.

12: mp 116.5 °C; ¹H NMR (CDCl₃) δ 1.10 (3H, t, *J* = 7.6 Hz), 2.31 (3H, s), 2.52 (2H, q, *J* = 7.6 Hz), 4.37 (2H, s), 5.20 (2H, s), 7.09–7.18 (2H, 2 overlapping triplets), 7.28–7.33 (5H, m), 7.34 (1H, d, *J* = 4 Hz), 7.59 (1H, t, *J* = 10 Hz), 7.70 (1H, d, *J* = 4 Hz), 8.2 (1H, br s), 8.22 (1H, d, *J* = 9.2 Hz), 8.31 (1H, d, *J* = 9.2 Hz); ¹³C NMR (CDCl₃) δ 10.7, 15.6, 17.5, 24.6, 65.4, 117.0, 117.3, 122.4, 123.0, 123.8, 125.5, 127.5, 128.0, 128.1, 128.6, 132.8, 133.5, 136.3, 137.0, 137.1, 137.9 (2), 141.3, 161.5. Anal. Calcd for C₂₆H₂₅NO₂: C, 81.43; H, 6.57; N, 3.65. Found: C, 81.63; H, 6.52; N, 3.78.

10a: mp 141–143 °C; ¹H NMR (CDCl₃) δ 1.05 (6H, t, *J* = 7.6 Hz), 2.30 (6H, s), 2.47 (4H, q, *J* = 7.5 Hz), 4.31 (4H, s), 5.20 (4H, s), 7.08 (2H, t, *J* = 9.8 Hz), 7.27–7.33 (10H, m), 7.47 (1H, s), 7.56 (1H, t, *J* = 9.8 Hz), 8.17 (2H, d, *J* = 10 Hz), 8.20 (2H, br s); ¹³C NMR (CDCl₃) δ 10.8, 15.6, 17.5, 24.5, 65.5, 117.1, 122.5, 123.9, 124.5, 127.6, 128.1 (2), 128.6, 132.7, 133.7, 136.9, 137.1, 138.5, 138.7, 161.5; HRMS (EI) calcd for C₄₂H₄₂N₂O₄ *m/z* 638.3144, found 638.3143. Anal. Calcd for C₄₂H₄₂N₂O₄: C, 78.97; H, 6.63; N, 4.38. Found: C, 79.02; H, 6.51; N, 4.47.

1,3-Bis(5-tert-butoxycarbonyl-3-ethyl-4-methyl-2-pyrrolylmethyl)azulene (10b). Azulene (438 mg) and *tert*-butyl 5-acetoxymethyl-4-ethyl-3-methylpyrrole-2-carboxylate⁵⁰ (2.14 g) were dissolved in 2-propanol (50 mL) and acetic acid (10 mL). The mixture was purged with nitrogen and refluxed overnight. The mixture was allowed to cool to room temperature, and the solvent was removed under reduced pressure. The residue was chromatographed on a silica column eluting with 60% dichloromethane–hexanes. The major blue band was collected and the solvent removed under reduced pressure. The residue was recrystallized from toluene, and upon suction filtration the product (1.027 g, 59%) was obtained as a baby blue powder: mp 150 °C dec; ¹H NMR (CDCl₃) δ 1.07 (6H, t, *J* = 7.4 Hz), 1.47 (18H, s), 2.26 (6H, s), 2.48 (4H, q, *J* = 7.4 Hz), 4.31 (4H, br s), 7.08 (1H, t, *J* = 9.8 Hz), 7.49 (1H, s), 7.56 (2H, t, *J* = 9.8 Hz), 8.11 (2H, br s), 8.18 (2H, d, *J* = 10 Hz); ¹³C NMR (CDCl₃) δ 10.7, 15.7, 17.6, 24.3, 28.7, 80.2, 118.7, 121.4, 124.7, 126.0, 131.6, 133.7, 137.0, 138.4, 138.7, 138.9, 161.5; HRMS (EI) calcd for C₃₆H₄₆N₂O₄ *m/z* 570.3458, found 570.3458. Anal. Calcd for C₃₆H₄₆N₂O₄: C, 75.76; H, 8.12; N, 4.91. Found: C, 75.30; H, 8.16; N, 4.60.

8,12,13,17-Tetraethyl-7,18-dimethylazuliporphyrin (1a). Tripyrranedicarboxylic acid **5a**^{35,51} (100 mg) was stirred in TFA (1 mL) under nitrogen for 10 min. The solution was diluted with dichloromethane (19 mL), 1,3-azulenedicarbaldehyde (41 mg) was added, and the resulting mixture was stirred overnight in the dark. Following neutralization by the dropwise addition of triethylamine, DDQ (51 mg) was added, and the resulting mixture was stirred for 1 h. The solution was washed with water and the organic phase evaporated under reduced pressure. Chromatographic separation of the residue was carried out on Grade III alumina, eluting with 5% methanol–chloroform. A deep green fraction was collected and evaporated under reduced pressure, and the residue recrystallized from chloroform–hexanes to give the azuliporphyrin (143 mg, 63%) as dark green crystals: mp >300 °C; UV–vis (1% Et₃N–CH₂Cl₂) λ_{max} (log ε) 354 (4.78), 396 (4.69), 444 (4.70), 472 (4.81), 622 nm (4.16); UV–vis (0.5% TFA–CH₂Cl₂) λ_{max} (log ε) 364 (4.95), 460 (5.08), 592 (3.85), 638 (4.46), 678 (4.17), 734 nm (3.82); ¹H NMR (TFA–CDCl₃) δ –2.98 (1H, s), –2.13 (1H, br s), –0.43 (2H, s), 1.67 (6H, t, *J* = 7.6 Hz), 1.78 (6H, t, *J* = 7.8 Hz), 3.50 (6H, s), 3.89 (8H, 2 overlapping quartets), 8.57 (1H, t, *J* = 9.6 Hz), 8.67 (2H, t, *J* = 9.6 Hz), 9.60 (2H, s), 10.06 (2H, d, *J* = 4.8 Hz), 10.45 (2H, s); ¹H NMR (pyridine-*d*₅) δ 1.65 (12H, t, *J* = 7.4 Hz), 3.08 (6H, s), 3.43–3.53 (8H, 2 overlapping quartets), 4.06 (1H, br s), 7.70 (2H, t, *J* = 9.4 Hz), 7.79 (1H, t,

J = 9.6 Hz), 8.49 (2H, s), 9.46 (2H, s), 9.64 (2H, d, *J* = 9.8 Hz); ¹H NMR (pyrrolidine-*d*₈–CDCl₃) δ –6.87 (1H, s), 1.76–1.83 (12H, 2 overlapping triplets), 3.06 (1H, tt, *J* = 2.8, 10 Hz), 3.53 (6H, s), 3.88 (4H, q, *J* = 7.6 Hz), 3.98 (4H, q, *J* = 7.6 Hz), 6.00 (2H, dd, *J* = 5.2, 9.2 Hz), 7.82 (2H, dd, *J* = 1.6, 9.0 Hz), 9.67 (2H, s), 9.88 (2H, s); ¹³C NMR (TFA–CDCl₃) δ 11.5, 16.1, 16.9, 19.6, 95.2, 110.2, 124.9, 128.1, 140.3, 142.0, 142.1, 142.2, 142.4, 144.5, 144.8, 146.2, 147.5, 154.1; HR MS (FAB) calcd for C₃₆H₃₇N₃ + H *m/z* 512.3066, found 512.3072. Anal. Calcd for C₃₆H₃₇N₃·H₂O: C, 81.62; H, 7.42; N, 7.93. Found: C, 81.23; H, 7.36; N, 7.86.

8,17-Diethyl-7,18-dimethyl-12,13-diphenylazuliporphyrin (1b). Tripyrrene **5b**^{17b} (303 mg) was reacted with 1,3-azulenedicarbaldehyde (103 mg) under the foregoing conditions. The crude product was chromatographed on Grade III alumina, eluting with 5% methanol–chloroform, and recrystallized from chloroform–hexanes to afford the porphyrin analogue (260 mg, 77%) as dark green crystals: mp >300 °C; UV–vis (5% Et₃N–CHCl₃) λ_{max} (log ε) 368 (4.78), 403 (4.70), 448 (4.67), 476 (4.78), 640 (3.69), 670 nm (3.70); UV–vis (5% TFA–CHCl₃) λ_{max} (log ε) 368 (4.64), 466 (4.82), 646 nm (3.93); ¹H NMR (2 drops TFA–CDCl₃) δ –2.96 (1H, s), –1.5 (1H, br s), –0.14 (2H, s), 1.59 (6H, t, *J* = 7.6 Hz), 3.49 (6H, s), 3.72 (4H, q, *J* = 7.7 Hz), 7.69–7.74 (6H, m), 7.81–7.85 (4H, m), 8.54 (1H, t, *J* = 9.6 Hz), 8.66 (2H, t, *J* = 9.6 Hz), 9.62 (2H, s), 10.05 (2H, d, *J* = 9.6 Hz), 10.46 (2H, s); ¹H NMR (pyrrolidine-*d*₈–CDCl₃) δ –6.82 (1H, s), 1.73 (6H, t, *J* = 7.6 Hz), 3.11 (1H, t, *J* = 5.2 Hz), 3.57 (6H, s), 3.88 (4H, q, *J* = 7.6 Hz), 6.05 (2H, dd, *J* = 5.2, 9.2 Hz), 7.57 (2H, t, *J* = 7.6 Hz), 7.65 (4H, t, *J* = 7.4 Hz), 7.86 (2H, d, *J* = 10 Hz), 7.94 (4H, d, *J* = 7.6 Hz), 9.80 (2H, s), 9.97 (2H, s); ¹³C NMR (TFA–CDCl₃) δ 11.6, 15.9, 19.6, 98.4, 110.0, 124.2, 128.6, 129.4, 129.7, 131.9, 132.0, 132.2, 140.5, 142.0, 142.3, 142.6, 142.9, 143.3, 146.4, 147.1, 154.4; HRMS (FAB) calcd for C₄₄H₃₇N₃ + H *m/z* 608.3066, found 608.3068. Anal. Calcd for C₄₄H₃₇N₃·1/4CHCl₃: C, 83.35; H, 5.88; N, 6.59. Found: C, 83.25; H, 5.30; N, 6.64.

12,13-Butano-8,17-diethyl-7,18-dimethylazuliporphyrin (1c). Tripyrrene **5c**³⁵ (100 mg) was reacted with 1,3-azulenedicarbaldehyde (40.6 mg) under the conditions described above. The product was purified by chromatography on Grade 3 basic alumina, eluting with chloroform. A deep green fraction was collected, evaporated under reduced pressure, and then recrystallized from chloroform–hexanes to give the azuliporphyrin (47 mg, 42%) as a dark blue powder: mp >300 °C; UV–vis (1% Et₃N–CHCl₃) λ_{max} (log ε) 354 (4.74), 396 (4.66), 444 (4.68), 472 (4.77), 614 (4.14), 662 nm (4.09); UV–vis (1% TFA–CHCl₃) λ_{max} (log ε) 368 (4.87), 464 (4.99), 642 nm (4.36); ¹H NMR (CDCl₃) δ 1.53 (6H, t, *J* = 7.6 Hz), 1.84 (1H, br s), 2.25–2.35 (4H, m), 2.96 (6H, s), 3.31 (4H, q, *J* = 7.6 Hz), 3.40–3.50 (4H, m), 7.61 (2H, t, *J* = 10 Hz), 7.71 (1H, t, *J* = 10 Hz), 7.92 (2H, s), 8.87 (2H, s), 9.23 (2H, d, *J* = 10 Hz); ¹H NMR (C₆D₆) δ 1.56 (6H, t, *J* = 7.6 Hz), 1.82 (4H, m), 2.86 (6H, s), 3.04 (4H, m), 3.27 (4H, q, *J* = 7.6 Hz), 6.84 (1H, t, *J* = 10 Hz), 6.97 (2H, obscured by solvent), 7.93 (2H, s), 8.76 (2H, d, *J* = 10 Hz), 8.85 (2H, s); ¹H NMR (pyridine-*d*₅, 50 °C) δ 1.66 (6H, t, *J* = 7.8 Hz), 2.06–2.12 (4H, m), 3.07 (6H, s), 3.34–3.38 (4H, m), 3.44 (4H, q, *J* = 7.6 Hz), 3.86 (1H, s), 7.69 (2H, t, *J* = 9.4 Hz), 7.78 (1H, t, obscured by solvent), 8.30 (2H, s), 9.45 (2H, s), 9.64 (2H, d, *J* = 10 Hz); ¹H NMR (TFA–CDCl₃) δ –2.55 (1H, s), –1.5 (1H, v br s), 0.4 (2H, br s), 1.65 (6H, t, *J* = 7.6 Hz), 2.40–2.48 (4H, m), 3.44 (6H, s), 3.79 (4H, q, *J* = 7.6 Hz), 3.8–3.86 (4H, m), 8.47 (1H, t, *J* = 10 Hz), 8.57 (2H, t, *J* = 9.6 Hz), 9.33 (2H, s), 9.95 (2H, d, *J* = 9.6 Hz), 10.32 (2H, s); ¹³C NMR (TFA–CDCl₃) δ 11.5, 15.9, 19.5, 22.5, 23.0, 94.8, 110.9, 124.4, 128.1, 140.4, 141.8, 142.3, 142.4, 142.5, 142.6, 144.6, 146.4, 147.8, 154.0; HR MS (ESI) calcd for C₃₆H₃₅N₃ + H *m/z* 510.2909, found 510.2909.

7,12,13,18-Tetraethyl-8,17-dimethylazuliporphyrin (14a). Azulitripyrrene analogue **10a** (100 mg) was stirred in TFA (2 mL) under nitrogen for 10 min. The reaction mixture was diluted with dichloromethane (100 mL), 3,4-diethylpyrrole-2,5-dicarbaldehyde^{35,52} (31 mg) was added, and the reac-

(50) Clezy, P. S.; Crowley, R. J.; Hai, T. T. *Aust. J. Chem.* **1982**, *35*, 411.

(51) Sessler, J. L.; Johnson, M. R.; Lynch, V. J. *Org. Chem.* **1987**, *52*, 4394.

tion mixture was stirred overnight in the dark. The solution was neutralized by the dropwise addition of triethylamine, DDQ (42 mg) was added, and the resulting mixture stirred for 1 h. The dark green solution was washed with water and the organic phase evaporated under reduced pressure. The residue was chromatographed on Grade III alumina, eluting with 2% methanol–chloroform. A deep green fraction was collected and evaporated under reduced pressure and the residue recrystallized from chloroform–hexanes. Suction filtration afforded the title azuliporphyrin (32 mg, 36%) as dark green crystals: mp >300 °C; UV–vis (1% Et₃N–CHCl₃) λ_{max} (log ϵ) 355 (4.74), 397 (4.67), 444 (4.67), 472 (4.76), 620 nm (4.13); UV–vis (2% TFA–CHCl₃) λ_{max} (log ϵ) 366 (4.89), 463 (4.99), 643 nm (4.36); UV–vis (5% pyrrolidine–CHCl₃) λ_{max} (log ϵ) 407 (4.98), 523 (4.24), 560 (4.08), 629 nm (3.50); ¹H NMR (TFA–CDCl₃) δ –2.87 (1H, s), –1.98 (1H, br s), –0.23 (2H, s), 1.73 (12H, 2 overlapping triplets), 3.37 (6H, s), 3.88 (4H, q), 3.95 (4H, q), 8.54 (1H, t, J = 9.2 Hz), 8.64 (2H, t, J = 9.6 Hz), 9.54 (2H, s), 10.02 (2H, d, J = 9.6 Hz), 10.40 (2H, s); ¹³C NMR (TFA–CDCl₃) δ 11.3, 16.4, 17.0, 19.7, 20.06, 95.3, 109.6, 123.7, 128.1, 135.9, 140.5, 140.9, 142.6, 144.2, 145.2, 146.5, 148.0, 148.9, 154.0; HR MS (ESI) calcd for C₃₆H₃₅N₃ + H m/z 512.3066, found 512.3067. Anal. Calcd for C₃₆H₃₇N₃·¹/₄CHCl₃: C, 80.40; H, 6.93; N, 7.76. Found: C, 80.50; H, 6.53; N, 7.60.

7,18-Diethyl-8,17-dimethyl-23-thiaazuliporphyrin (14b). **Method A.** Azulitripyrrane analogue **10b** (100 mg) was stirred in TFA (1 mL) under nitrogen for 10 min. The reaction mixture was diluted with dichloromethane (100 mL), 2,5-thiophenedicarbaldehyde (41 mg) was added, and the reaction mixture was stirred overnight in the dark. The solution was neutralized by the dropwise addition of triethylamine, DDQ (50 mg) was added, and the resulting mixture was stirred for 1 h. The dark green solution was washed with water, and the organic phase evaporated under reduced pressure. The residue was chromatographed on Grade III alumina, eluting with chloroform. A deep green fraction was collected and evaporated under reduced pressure. Recrystallization from chloroform–hexanes gave the porphyrinoid (29.2 mg, 33%) as dark green crystals: mp >300 °C; UV–vis (5% Et₃N–CH₂Cl₂) λ_{max} (log ϵ) 372 (4.74), 384 (4.72), 448 (4.59), 477 (4.66), 632 (4.07), 672 nm (4.10); UV–vis (5% TFA–CH₂Cl₂) λ_{max} (log ϵ) 385 (4.54), 468 (4.92), 601 (3.78), 661 nm (4.14); ¹H NMR (CDCl₃) δ 1.61 (6H, t, J = 7.8 Hz), 2.76 (1H, br s), 2.88 (6H, s), 3.45 (4H, q, J = 7.7 Hz), 7.80–7.92 (3H, m), 8.82 (2H, s), 9.05 (2H, s), 9.24 (2H, s), 9.52 (2H, d, J = 9.2 Hz); ¹H NMR (C₆D₆) δ 1.56 (6H, t, J = 7.4 Hz), 2.66 (6H, s), 3.34 (4H, q, J = 8 Hz), 6.89 (1H, t), 6.97 (2H, obscured by solvent), 8.46 (2H, s), 8.83 (2H, s), 8.94 (2H, d, J = 9.6 Hz), 9.13 (2H, s); ¹H NMR (pyridine-*d*₅) δ 1.59 (6H, t, J = 7.2 Hz), 2.89 (6H, s), 3.20 (1H, s), 3.52 (4H, q, J = 7.7 Hz), 7.78–7.93 (3H, m), 9.13 (2H, s), 9.44 (2H, s), 9.82 (2H, s), 9.98 (2H, d, J = 10 Hz); ¹H NMR (10 drops pyrrolidine-*d*₈–CDCl₃) δ –5.42 (1H, s), 1.62 (6H, t, J = 7.6 Hz), 2.96 (1H, t), 3.24 (6H, s), 3.72 (4H, q, J = 7.5 Hz), 5.87 (2H, dd, J = 5.2, 9.2 Hz), 7.83 (2H, d, J = 9.2 Hz), 9.67 (2H, s), 9.85 (2H, s), 10.18 (2H, s); ¹H NMR (TFA–CDCl₃) δ –3.44 (1H, s), –1.5 (2H, v br s), 1.79 (6H, t, J = 7.8 Hz), 3.49 (6H, s), 4.05 (4H, q, J = 7.7 Hz), 8.78 (1H, t, J = 9.6 Hz), 8.92 (2H, t, J = 10 Hz), 9.99 (2H, s), 10.38 (2H, d, J = 10 Hz), 10.60 (2H, s), 10.86 (2H, s); ¹³C NMR (TFA–CDCl₃) δ 11.4, 16.6, 20.2, 111.7, 111.9, 130.4, 138.5, 139.8, 141.1, 141.9, 145.3, 148.4, 148.7, 150.1, 150.3, 157.2, 161.0; HRMS (FAB) calcd for C₃₂H₂₈N₂S + H m/z 473.2051, found 473.2049. Anal. Calcd for C₃₂H₂₈N₂S·²/₅CHCl₃: C, 74.78; H, 5.50; N, 5.38. Found: C, 74.78; H, 5.61; N, 5.36.

Method B. Azulitripyrrane **10b** (101.3 mg) was stirred in TFA (2 mL) under nitrogen for 10 min. The reaction mixture was diluted with dichloromethane (100 mL), 2,5-thiophenedicarbaldehyde (41 mg) was added, and the reaction mixture was stirred overnight in the dark. The solution was vigorously

shaken with 0.1% aqueous ferric chloride solution (150 mL) for 10 min. The organic layer was separated and washed with water, 5% sodium bicarbonate solution, and water. The organic phase was dried over sodium sulfate and evaporated under reduced pressure and the residue chromatographed and recrystallized as before. The thiaazuliporphyrin (40.4 mg, 45%) was isolated as dark green crystals: mp >300 °C.

7,18-Diethyl-8,17-dimethyl-23-selenaazuliporphyrin (14c). Azulitripyrrane **10b** (100 mg) was reacted with 2,5-selenophenedicarbaldehyde (35 mg) by method B, as described above. The crude product was purified by chromatography on Grade 3 neutral alumina, eluting with chloroform. A dark green band was collected and evaporated to dryness under reduced pressure and the residue recrystallized from chloroform–hexanes to give the selenaazuliporphyrin (24.2 mg, 27%) as a deep green powder: mp >300 °C; UV–vis (1% Et₃N–CHCl₃) λ_{max} (log ϵ) 363 (4.73), 399 (4.66), 449 (4.62), 476 (4.67), 627 (4.14), 666 nm (4.15); UV–vis (5% TFA–CHCl₃) λ_{max} (log ϵ) 368 (4.57), 382 (4.55), 494 (4.97), 625 (3.90), 682 nm (4.07); UV–vis (25% pyrrolidine–CHCl₃) λ_{max} (log ϵ) 446 (4.95), 474 (4.83), 600 nm (4.20); ¹H NMR (CDCl₃) δ 1.61 (6H, t, J = 7.6 Hz), 2.86 (6H, s), 3.04 (1H, s), 3.43 (4H, q, J = 7.6 Hz), 7.84 (2H, t, J = 9.2 Hz), 7.93 (1H, t, J = 9.8 Hz), 8.93 (2H, s), 9.18 (2H, s), 9.21 (2H, s), 9.51 (2H, d, J = 9.2 Hz); ¹H NMR (C₆D₆) δ 1.53 (6H, t, J = 7.8 Hz), 2.62 (6H, s), 3.30 (4H, q, J = 7.6 Hz), 3.53 (1H, s), 6.87–7.1 (3H, obscured by solvent), 8.69 (2H, s), 8.93 (2H, d, J = 9.2 Hz), 8.99 (2H, s), 9.07 (2H, s); ¹H NMR (pyridine-*d*₅) δ 1.57 (6H, t, J = 7.4 Hz), 2.86 (6H, s), 3.40 (1H, s), 3.48 (4H, q, J = 7.6 Hz), 7.85 (2H, t, J = 9.4 Hz), 7.94 (1H, t, J = 9.2 Hz), 9.27 (2H, s), 9.56 (2H, s), 9.78 (2H, s), 9.98 (2H, d, J = 10 Hz); ¹H NMR (20 drops pyrrolidine-*d*₈–CDCl₃) δ –4.75 (1H, s), 1.55 (6H, t, partially obscured by water peak), 2.84 (1H, t, J = 5.2 Hz), 3.03 (6H, s), 3.48–3.56 (4H, m), 5.68 (2H, dd, J = 5.2, 9.2 Hz), 7.72 (2H, d, J = 10 Hz), 9.64 (2H, s), 9.67 (2H, s), 10.10 (2H, s); ¹H NMR (TFA–CDCl₃) δ –2.61 (1H, s), –1.62 (2H, br s), 1.78 (6H, t, J = 7.4 Hz), 3.48 (6H, s), 4.07 (4H, q, J = 7.6 Hz), 8.81 (1H, t, J = 9.4 Hz), 8.93 (2H, t, J = 9.8 Hz), 9.94 (2H, s), 10.38 (2H, d, J = 8.8 Hz), 10.73 (2H, s), 10.83 (2H, s); ¹³C NMR (TFA–CDCl₃) δ 11.2, 16.4, 20.2, 112.7, 115.0, 120.7, 129.4, 129.5, 138.1, 140.0, 140.1, 141.6, 141.7, 144.7, 148.4, 151.3, 151.4, 151.6, 156.3, 158.5; HRMS (ESI) calcd for C₃₂H₂₈N₂Se + H m/z 521.1496, found 521.1517. Anal. Calcd for C₃₂H₂₈N₂Se·¹/₂₀CHCl₃: C, 73.25; H, 5.38; N, 5.33. Found: C, 73.20; H, 5.23; N, 5.29.

Synthesis of Oxabenzocarbaporphyrins 15a–c. Azulitripyrrane **10b** (100 mg) was stirred in TFA (1 mL) under nitrogen for 10 min. The reaction mixture was diluted with dichloromethane (19 mL), and 2,5-furandicarbaldehyde (40 mg) was added immediately. The reaction mixture was purged with nitrogen and stirred overnight in the dark. The solution was neutralized with triethylamine, DDQ (50 mg) was added, and the resulting mixture was stirred for 1 h. The solution was washed with 2 M aqueous hydrochloric acid. The organic phase was separated and the solvent removed under reduced pressure. The residue was chromatographed on a silica column, eluting first with chloroform and then gradually increasing the polarity to 5% methanol–chloroform. A deep green fraction was collected and evaporated under reduced pressure. The residue was recolumned using flash chromatography eluting with 5% methanol–chloroform. Three separate green fractions corresponding to oxabenzocarbaporphyrins **15a–c** were collected; the order of elution was **15a**, **15c**, then **15b**. Recrystallization from chloroform–hexanes gave the oxabenzocarbaporphyrins as dark green crystals.

15a. HCl: 5.8 mg (7.5%); mp >300 °C; UV–vis (5% Et₃N–CHCl₃) λ_{max} (log ϵ) 372 (4.61), 430 (4.79), 522 (4.11), 555 (3.83), 620 (3.76), 681 nm (3.34); UV–vis (2% TFA–CHCl₃) λ_{max} (log ϵ) 393 (4.80), 410 (4.72), 477 (4.40), 573 (4.00), 609 nm (4.07); UV–vis (5% TFA–CHCl₃) λ_{max} (log ϵ) 393 (4.81), 411 (4.77), 573 (3.97), 610 nm (4.07); ¹H NMR (CDCl₃) δ –6.72 (1H, s), –2.72 (2H, br s), 1.77 (6H, t, J = 7.6 Hz), 3.58 (6H, s), 4.09 (4H, q, J = 7.6 Hz), 7.68–7.73 (2H, m), 8.63–8.67 (2H, m),

(52) Tardieux, C.; Bolze, F.; Gros, C. P.; Guillard, R. *Synthesis* **1998**, 267.

9.85 (2H, s), 10.15 (2H, s), 10.36 (2H, s); ^{13}C NMR (CDCl_3) δ 11.7, 17.3, 20.2, 94.8, 105.7, 121.7, 128.4, 134.0, 137.3, 138.9, 140.7, 142.0, 142.2, 152.7; HRMS (EI) calcd for $\text{C}_{31}\text{H}_{28}\text{N}_2\text{O}$ m/z 444.2201, found 444.2201.

15b. HCl: 4.7 mg (5.7%); mp >300 °C; UV–vis (5% Et_3N – CHCl_3) λ_{max} (log ϵ) 432 (4.93), 523 (4.13), 557 (4.03), 621 (3.82), 683 nm (3.52); UV–vis (5% TFA– CHCl_3) λ_{max} (log ϵ) 392 (4.65), 434 (4.97), 472 (4.61), 566 (4.02), 607 (4.21), 646 nm (3.36); ^1H NMR (CDCl_3) δ –6.40 (1H, s), –1.64 (2H, br s), 1.75–1.81 (6H, t, J = 7.6 Hz), 3.53 (6H, s), 4.05 (4H, q, J = 7.6 Hz), 8.20 (1H, d, J = 7.6 Hz), 8.79 (1H, d, J = 8.0 Hz), 9.15 (1H, s), 9.79 (2H, s), 10.09 (2H, AB q), 10.34 (1H, s), 10.40 (1H, s), 10.43 (1H, s); HRMS (EI) calcd for $\text{C}_{32}\text{H}_{28}\text{N}_2\text{O}_2$ m/z 472.2150, found 472.2143.

15c. HCl: 1.4 mg (1.7%); mp >300 °C; UV–vis (5% Et_3N – CHCl_3) λ_{max} (rel int.) 371 (0.46), 431 (1.00), 525 (0.17), 558 (0.12), 620 (0.08), 681 nm (0.05); UV–vis (5% TFA– CHCl_3) λ_{max} (rel int.) 390 (0.61), 435 (1.00), 476 (0.46), 576 (0.13), 604 (0.15), 657 nm (0.04); ^1H NMR (CDCl_3) δ –6.39 (1H, s), –1.8, –1.6 (2H, 2 overlapping broad singlets), 1.76 (6H, 2 overlapping triplets), 3.56 (6H, s), 4.09 (2H, q, J = 7 Hz), 4.17 (2H, q, J = 7 Hz), 7.90 (1H, t, J = 7.6 Hz), 8.19 (1H, d, J = 7.5 Hz), 8.95 (1H, d, J = 7.5 Hz), 9.81 (2H, s), 10.12–10.16 (2H, AB q), 10.42 (1H, s), 10.87 (1H, s), 12.03 (1H, s); HRMS (EI) calcd for $\text{C}_{32}\text{H}_{28}\text{N}_2\text{O}_2$ m/z 472.2151, found 472.2149.

Oxidative Ring Contraction of Thiazuliporphyrin 14b.

Method A. Potassium *tert*-butoxide (1.0 M) in *tert*-butyl alcohol (100 mL) was added to a solution of thiazuliporphyrin (101 mg) in dichloromethane (100 mL), and the resulting stirred mixture was purged with nitrogen for 10 min. A solution of *tert*-butyl hydroperoxide in decane (5 M, 150 μL) was added and the resulting solution stirred under nitrogen in the dark at room temperature for 4 h. The solution was washed with water ($\times 2$), dried over sodium sulfate, and evaporated under reduced pressure. The residues were chromatographed on a flash silica column, eluting with dichloromethane. The first major orange band was collected, the solvent evaporated, and the residue recrystallized from chloroform–hexanes to give thiabenzocarbaporphyrin **25a** (9.3 mg, 9.5%) as a black powder: mp >300 °C; UV–vis (1% Et_3N – CHCl_3) λ_{max} (log ϵ) 390 (4.54), 434 (4.84), 530 (4.11), 557 (sh, 3.88), 625 (3.72), 684 nm (3.11); UV–vis (0.02% TFA– CHCl_3) λ_{max} (log ϵ) 448 (4.76), 495 (4.37), 620 (3.93), 688 nm (3.41); ^1H NMR (CDCl_3) δ –5.90 (1H, s), –5.08 (1H, br s), 1.79 (6H, t, J = 7.6 Hz), 3.37 (6H, s), 3.87 (4H, q, J = 7.6 Hz), 7.76–7.79 (2H, m), 8.83–8.86 (2H, m), 9.72 (2H, s), 10.06 (2H, s), 10.11 (2H, s); ^1H NMR (TFA– CDCl_3) δ –6.87 (1H, s), –5.34 (2H, br s), 1.84 (6H, br t), 3.67 (6H, s), 4.11 (4H, br q), 7.79–7.86 (2H, m), 8.74–8.82 (2H, m), 10.29 (2H, s), 10.46 (2H, s), 10.96 (2H, s); ^{13}C NMR (CDCl_3) δ 11.4, 17.6, 19.8, 104.9, 107.5, 116.1, 120.6, 127.1, 131.7, 134.4, 136.9, 140.5, 142.7, 143.9; ^{13}C NMR (TFA– CDCl_3) δ 11.9, 17.2, 20.1, 105.2, 108.9, 114.0, 122.3, 129.7, 136.2, 138.1, 139.7, 141.3, 141.5, 141.9, 142.0, 143.8; HRMS (EI) calcd for $\text{C}_{31}\text{H}_{28}\text{N}_2\text{S}$ m/z 460.1973, found 460.1970.

Method B. Potassium hydroxide (475 mg) in methanol (60 mL) was added to a solution of thiazuliporphyrin (60.3 mg) in dichloromethane (60 mL), and the resulting stirred mixture was purged with nitrogen for 10 min. A solution of *tert*-butyl hydroperoxide in decane (5 M, 90 μL) was added and the resulting solution stirred under nitrogen in the dark at room temperature for 2 h. The solution was washed with water ($\times 2$), dried over sodium sulfate, and evaporated under reduced pressure. The residues were chromatographed on a flash silica column, eluting initially with dichloromethane and then 75% chloroform–dichloromethane. The major orange band was collected, the solvent evaporated, and the residue recrystallized from chloroform–hexanes to give a purple powder (33.5 mg) corresponding to a mixture of **25a** and **25b**. These derivatives could not be separated using flash chromatography. Although the ratio of the two major products varied, the ratio of **25b** to **25a** was usually approximately 2:1.

Oxidative Ring Contraction of Selenazuliporphyrin

14c. Method A. Using method A (above), selenazuliporphyrin

(42.3 mg) was reacted with *tert*-butyl hydroperoxide (5 M in hexane, 70 μL) for 2 h. The crude product was run through a flash silica column, eluting with 30/70 hexanes/dichloromethane. An orange band eluted, and this was evaporated under reduced pressure and the residue recrystallized from chloroform–hexanes to give selenabenzocarbaporphyrin **26a** (4.2 mg, 10.2%) as black crystals: mp 282–284 °C dec; UV–vis (1% Et_3N – CHCl_3) λ_{max} (log ϵ) 436 (4.93), 533 (4.11), 565 (3.94), 630 nm (3.77); UV–vis (0.1% TFA– CHCl_3) λ_{max} (log ϵ) 314 (4.44), 379 (4.39), 469 (4.85), 511 (4.51), 637 nm (4.02); UV–vis (10% TFA– CHCl_3) λ_{max} (log ϵ) 308 (4.37), 332 (4.31), 445 (4.86), 633 nm (4.11); ^1H NMR (CDCl_3 , 30 °C) δ –5.38 (1H, s), –4.86 (1H, br s), 1.79 (6H, t, J = 7.6 Hz), 3.38 (6H, s), 3.89 (4H, q, J = 7.6 Hz), 7.75–7.78 (2H, m), 8.82–8.84 (2H, m), 9.96 (2H, s), 10.16 (2H, s), 10.43 (2H, s); ^1H NMR (trace TFA– CDCl_3) δ –5.57 (1H, s), –4.31 (2H, br s), 1.83 (6H, t, J = 7.6 Hz), 3.61 (6H, s), 4.10 (4H, q, J = 7.6 Hz), 7.72–7.75 (2H, m), 8.68–8.71 (2H, m), 10.09 (2H, s), 10.42 (2H, s), 10.99 (2H, s); ^{13}C NMR (CDCl_3) δ 11.3, 17.5, 19.9, 106.1, 111.2, 116.4, 120.6, 127.0, 133.5, 134.0, 135.9, 142.8, 143.8, 146.0; ^{13}C NMR (trace TFA– CDCl_3) δ 11.7, 17.1, 20.1, 105.5, 112.1, 113.7, 121.9, 129.1, 136.9, 137.3, 140.1, 140.9, 142.1, 142.6, 144.3, 151.8; HR MS (ESI) calcd for $\text{C}_{31}\text{H}_{28}\text{N}_2\text{Se} + \text{H}$ 509.1496, found 509.1488.

Method B. Selenazuliporphyrin **14c** (43.1 mg) was reacted with *tert*-butyl hydroperoxide (5 M in hexane, 70 μL) for 4 h using method B (above). The crude product was run through a flash silica column, eluting with 30/70 hexanes/dichloromethane. After the first orange band corresponding to **26a** had eluted, the polarity was increased to straight dichloromethane. After some minor impurity bands had eluted, a second orange band corresponding to formyl selenabenzocarbaporphyrin **26b** was collected. The two major fractions were evaporated and recrystallized from chloroform–hexanes. The first band gave selenabenzocarbaporphyrin **26a** (6.7 mg, 16%) as dark purple needles that gave spectroscopic properties identical to those of the compound prepared by method A. The second major fraction afforded the aldehyde **26b** (9.6 mg, 22%) as shiny black crystals: mp 281–282 °C dec; UV–vis (1% Et_3N – CHCl_3) λ_{max} (log ϵ) 439 (5.04), 540 (4.10), 571 (4.10), 628 (3.81), 687 nm (3.28); UV–vis (1% TFA– CHCl_3) λ_{max} (log ϵ) 311 (4.46), 334 (4.42), 384 (4.37), 464 (5.00), 500 (4.65), 632 nm (4.09); ^1H NMR (CDCl_3 , 20 °C) δ –6.48 (1H, s), –6.34 (1H, br s), 1.69 (6H, br m), 3.24 (3H, s), 3.26 (3H, s), 3.65–3.75 (4H, m), 8.14 (1H, dd, J = 1.2, 7.6 Hz), 8.97 (1H, br d), 9.60 (2H, br), 9.74 (2H, s), 10.08 (1H, s), 10.10 (1H, s), 10.42 (1H, s); ^1H NMR (trace TFA– CDCl_3 , 20 °C) δ –5.35 (1H, s), –4.81 (2H, br s), 1.89 (6H, t, J = 7.6 Hz), 3.70 (3H, s), 3.71 (3H, s), 4.18–4.27 (4H, 2 overlapping quartets), 8.46 (1H, d, J = 7.6 Hz), 9.10 (1H, d, J = 7.2 Hz), 9.55 (1H, s), 10.27 (2H, s), 10.34 (1H, s), 10.73 (1H, s), 10.82 (1H, s), 11.19 (2H, s, resolves into 2 singlets at 30 °C); ^{13}C NMR (trace TFA– CDCl_3) δ 11.7 (2), 17.0, 20.1, 20.2, 106.7, 106.9, 110.4, 112.9, 113.0, 113.2, 114.2, 116.1, 118.9, 122.6, 122.7, 134.2, 135.8, 137.7, 137.9, 138.0, 138.2, 138.6, 140.5, 140.8, 142.5, 142.9, 143.1, 146.1, 146.3, 148.4, 151.6, 151.8, 196.9; HR MS (ESI) calcd for $\text{C}_{32}\text{H}_{28}\text{N}_2\text{OSe} + \text{H}$ 537.1445, found 537.1435.

Oxidative Ring Contraction of Azuliporphyrin 1a.

Method A. Azuliporphyrin **1a** (40.0 mg) was reacted with *tert*-butyl hydroperoxide (5 M in hexane, 78 μL) in the presence of potassium *tert*-butoxide under the conditions described for method A (above) for 2 h. The crude product was run through a flash silica column, eluting with 20/80 hexanes/dichloromethane. A major orange-brown band eluted, and this was evaporated under reduced pressure and the residue recrystallized from chloroform–hexanes to give benzocarbaporphyrin **4**^{17a,b} (12 mg, 31%) as a fluffy brown solid, mp >300 °C. This material was indistinguishable from the carbaporphyrin obtained from tripyrrane **5a** and diformylindene.¹⁷ A minor more polar band corresponding to <5% of **9a** was also collected.

Method B. Azuliporphyrin **1a** (40.0 mg) was reacted with *tert*-butyl hydroperoxide (5 M in hexane, 78 μL) in the presence of potassium hydroxide for 4 h using method B (above). The

crude product was run through a flash silica column, eluting with 20/80 hexanes/dichloromethane. Two major orange-brown bands were collected, together with a minor band of intermediary polarity. The first band was evaporated down and the residue recrystallized from chloroform–methanol to give benzocarbaporphyrin **4**^{17a,b} (7.6 mg, 19%) as a brown solid, mp >300 °C. The more polar band was also evaporated down and recrystallized from chloroform–methanol to give the aldehyde **9a** (14.6 mg, 35%) as purple crystals: mp >300 °C; UV–vis (1% Et₃N–CHCl₃) λ_{max} (log ϵ) 375 (4.53), 433 (5.26), 489 (3.98), 519 (4.17), 557 (4.39), 605 (3.87), 668 nm (3.24); ¹H NMR (400 MHz, CDCl₃) δ –7.55 (1H, s), –4.77 (2H, br s), 1.76–1.82 (6H, two overlapping triplets), 1.85 (6H, t, J = 7.6 Hz), 3.40 (3H, s), 3.43 (3H, s), 3.88–3.99 (8H, m), 7.99 (1H, d, J = 8 Hz), 8.47 (1H, d, J = 8 Hz), 8.85 (1H, s), 9.52 (2H, s), 9.58 (1H, s), 9.60 (1H, s), 10.29 (1H, s); ¹³C NMR (CDCl₃) δ 11.4 (2), 17.5, 18.7, 19.6 (2), 20.1, 95.3, 95.4, 98.8, 110.6, 120.2, 120.6, 128.9, 130.8, 131.2, 132.9, 133.0, 134.5, 134.9, 135.9, 136.0, 137.7,

141.0, 144.6, 144.7, 146.1, 153.2, 153.3, 193.0; HR MS (EI) calcd for C₃₆H₃₇N₃O m/z 527.2936, found 527.2933. Anal. Calcd for C₃₆H₃₇N₃O·¹/₈CHCl₃: C, 79.96; H, 6.89; N, 7.74. Found: C, 80.23; H, 6.34; N, 7.80.

Acknowledgment. This material is based upon work supported by the National Science Foundation under Grant Nos. CHE-9732054 and CHE-0134472 and the Petroleum Research Fund, administered by the American Chemical Society.

Supporting Information Available: UV–vis, ¹H NMR, ¹³C NMR, and mass spectra for selected compounds are provided. This material is available free of charge via the Internet at <http://pubs.acs.org>.

JO0402531